NOVEL INSIGHTS INTO DNA DOUBLE-STRAND BREAK REPAIR

AND ITS CANCER IMPLICATIONS

APPROVED BY SUPERVISORY COMMITTEE

Sandeep Burma, Ph.D. (Mentor)
Associate Professor, Radiation Oncology

Robert Bachoo, M.D., Ph.D.
Associate Professor, Neurology and Neurotherapeutics

Rolf Brekken, Ph.D.
Professor, Surgery

Jerry Shay, Ph.D. (Chairman)
Professor, Cell Biology

DEDICATION

I would like to dedicate this work to all of my family members who have battled cancer.

NOVEL INSIGHTS INTO DNA DOUBLE-STRAND BREAK REPAIR AND ITS CANCER IMPLICATIONS

by

MOLLY CATHERINE HARDEBECK

DISSERTATION

Presented to the Faculty of the Graduate School of Biomedical Sciences

The University of Texas Southwestern Medical Center

In Partial Fulfillment of the Requirements

For the Degree of

DOCTOR OF PHILOSOPHY

The University of Texas Southwestern Medical Center

Dallas, Texas

August, 2016

ACKNOWLEDGEMENTS

First, I would like to thank God for this amazing experience and for allowing me to share this experience with so many wonderful people. God was with me both during the joyous times and the struggles, and I am forever grateful for this experience which allowed me to grow closer to Him.

I would like to thank my husband, Matthew. I could have never survived this experience without you. You are my support on this journey every single day. Thank you for your love and constant encouragement and for never letting me give up. Thank you also to our newest love, Vincent Paul, for the smiles and indescribable joy you bring to our lives.

Thank you to all of my family, especially my parents, Tony and Jan. They believed in me and supported me even in the lowest times. Their love means the world to me, and I would not be here without them.

I would like to acknowledge my mentor, Sandeep Burma, for all of his guidance, support, and encouragement. His passion and enthusiasm for science is contagious. I am thankful for all of the opportunities that otherwise would not have been possible without him.

I would like to thank my thesis committee: Dr. Jerry Shay, Dr. Robert Bachoo, and Dr. Rolf Brekken. Their experimental feedback, support, and mentorship were invaluable to my success.

I would like to thank my current and former lab mates: Bipasha Mukherjee, Nozomi Tomimatsu, Xiaohuan Gao, Brian McEllin, Cristel Camacho, Mariya Ilcheva, Carlos Gil del Alcazar, and Pavlina Todorova. They provided an incredible amount of scientific support and more importantly, friendship. This experience would not have been the same without them.

NOVEL INSIGHTS INTO DNA DOUBLE-STRAND BREAK REPAIR AND ITS CANCER IMPLICATIONS

Molly Catherine Hardebeck

The University of Texas Southwestern Medical Center, 2016

Supervising Professor: Sandeep Burma, Ph.D.

ABSTRACT

Despite the aggressive treatment with DNA damage-inducing agents, glioblastomas (GBM) inevitably develop therapy resistance, leading to relapse and patient mortality. Cancer cells that survive therapy acquire additional damage-induced oncogenic changes that likely facilitate therapy resistance and tumor recurrence. To understand which damage-induced oncogenic alterations may promote tumor recurrence, we previously irradiated brains of mice harboring deletions of key tumor suppressors frequently lost in GBM. The most significant acquired alteration was amplification of the Met tyrosine kinase. We find that Met-expressing cells display cancer stem cell properties, augmented tumorigenesis, up-regulation of numerous DNA damage response (DDR) proteins, and an extended G2/M arrest. We hypothesize that Met expression drives therapy resistance and may be a potential target for radiosensitizing GBM. An alternative sensitization approach could involve direct inhibition of key DDR proteins, specifically in the homologous recombination (HR) double-strand break (DSB) repair pathway

which is implicated in radioresistance of GBM stem cells. One indispensable step of HR is DNA-end resection, primarily executed by the exonuclease EXO1. We found that an EXO1 construct lacking the C-terminus and containing only the nuclease domain does not localize to DSBs, causing severe resection and repair defects. We hypothesized that the C-terminus of EXO1 serves as a platform for proteins to regulate EXO1's function. We found that the C-terminus interacts with BLM helicase, and it contains four Ser/Thr-Pro sites that are phosphorylated by CDKs1/2 to promote resection. We are currently examining whether CDK phosphorylation of EXO1 modulates the duration of the G2/M checkpoint since proper DNA repair requires a halt in the cell cycle. We are using CRISPR technology to generate EXO1 knock-out cells that will be complemented with WT or CDK-mutant EXO1 for checkpoint studies. We hypothesize that CDK phosphorylation of EXO1 serves to regulate resection and sustain the G2/M checkpoint. To further elucidate the role of EXO1 in maintaining genomic stability, we examined a cancer-associated SNP in EXO1 and found that it causes resection and DSB repair defects which may contribute to genomic instability and cancer progression. Overall, we provide novel insights into multiple aspects of DSB repair and identify potential targets for cancer therapy.

TABLE OF CONTENTS

PUBLICATIONS

Chang J, Varghese DS, **Gillam MC**, Peyton M, Modi B, Schiltz RL, Girard L, Martinez ED. Differential response of cancer cells to HDAC inhibitors trichostatin A and depsipeptide. *British Journal of Cancer* 2012; 106(1):116-25.

Gil del Alcazar CR, **Hardebeck MC**, Mukherjee B, Tomimatsu N, Gao X,Yan J, Xie XJ, Bachoo R, Li L, Habib AA, Burma S. Inhibition of DNA double-strand break repair by the dual PI3K/mTOR inhibitor NVP-BEZ235 as a strategy for radiosensitization of glioblastoma. *Clinical Cancer Research* 2014; 20(5):1235-48.

Tomimatsu N, Mukherjee B, **Hardebeck MC**, Ilcheva M, Camacho CV, Harris JL, Porteus M, Llorente B, Khanna KK, Burma S. Phosphorylation of EXO1 by CDKs 1 and 2 regulates DNA end resection and repair pathway choice. *Nature Communications* 2014; 5:3561.

Camacho CV, Todorova P, **Hardebeck MC**, Gil del Alcazar CR, Ilcheva M, Tomimatsu N, Mukherjee B, McEllin B, Vemireddy V, Hatanpaa K, Story MD, Habib AA, Murty VV, Bachoo R, Burma S. DNA double-strand breaks cooperate with loss of Ink4 and Arf tumor suppressors to generate glioblastomas with frequent Met amplification. *Oncogene* 2015, 34(8):1064-72.

Collaboration with Dr. Ram Mani. Targeting DNA repair in advanced prostate cancer. [Manuscript in preparation].

LIST OF FIGURES

LIST OF APPENDICES

LIST OF ABBREVIATIONS

6-TG	6-thioguanine
53bp1	p53-binding protein 1
AAVS1	Adeno-associated virus integration site 1
aCHG	array comparative genomic hybridization
AKT	Protein kinase B
ARF	Adenosine diphosphate-ribosylation factor 1
ATM	Ataxia telangiectasia mutated
ATR	Ataxia telangiectasia and Rad3-related protein
ATRIP	Ataxia telangiectasia and Rad3-related protein interacting protein
bFGF	basic fibroblast growth factor
B-gal	beta-galactosidase
BER	base excision repair
BLM	Bloom syndrome, RecQ helicase-like
bp	base pairs
BRCA1	Breast cancer 1, early onset
BRCA2	Breast cancer 2, early onset

BrdU	bromodeoxyuridine
C-terminus	carboxyl-terminus
CDC7	Cell division cycle 7-related protein kinase
CDC25a/c	Cell division cycle 25A/C
CDK	Cyclin-dependent kinase
CHK1	Checkpoint kinase 1
CHK2	Checkpoint kinase 2
CMV	cytomegalovirus
CPT	camptothecin
CtIP	C-terminal binding protein-interacting protein
CRISPR/Cas9	clustered regularly interspaced short palindromic repeats/CRISPR associated protein 9
DDR	DNA damage response
DMEM	Dulbecco's Modified Eagle Medium
DNA	deoxyribonucleic acid
DNA2	DNA replication ATP-dependent helicase/nuclease 2
DNA-PK	DNA-dependent protein kinase
DNA-PKcs	DNA-dependent protein kinase catalytic subunit

DSB	double-strand break
DTT	dithiothreitol
EDTA	ethylenediaminetetraacetic acid
EF-1 α	elongation factor 1-alpha
EGF	Epidermal growth factor
EGFR	Epidermal growth factor receptor
EGFRvIII	Epidermal growth factor receptor variant III
EME1	Essential meiotic structure-specific endonuclease 1
ERBB2	Receptor tyrosine-protein kinase avian erythroblastosis oncogene B-2
EXO1	Exonuclease 1
EZH2	Enhancer of zeste homolog 2
FAK	Focal adhesion kinase
FGF	Fibroblast growth factor
FISH	fluorescence in situ hybridization
	flox
GAB1	Growth factor receptor-bound protein 2-associated-binding protein 1
GABRA1	Gamma-aminobutyric acid A receptor, alpha 1

GBM	glioblastoma
GEN1	GEN1 Holliday junction 5’ flap endonuclease
GRB2	Growth factor receptor-bound protein 2
GWAS	genome-wide association study
gRNA	guide ribonucleic acid
Gy	gray
HPRT	hypoxanthine-guanine phosphoribosyltransferase
HDAC	histone deacetylase
HGF	Hepatocyte growth factor
HNPCC	hereditary nonpolyposis colorectal cancer
HR	homologous recombination
IDH1/2	isocitrate dehydrogenase 1/2
Ink4	Inhibitor of cyclin-dependent kinase type 4
IR	ionizing radiation
KAP-1	Krüppel-associated box-associated protein 1
kb	kilobase
LIG4	DNA Ligase 4

MAPK	Mitogen-activated protein kinase
MELK	Maternal embryonic leucine zipper kinase
MET	Hepatocyte growth factor receptor
mg	milligram
MG132	carbobenzoxy-Leu-Leu-leucinal
mL	milliliter
MLH1	Mutator L homolog 1
mm	millimeter
mM	millimolar
MMR	mismatch repair
MRE11	Meiotic recombination 11
MRN	MRE11-Rad50-NBS1
MSH2	Mutator S homolog 2
MSH3	Mutator S homolog 3
MUS81	Methansulfonate and ultraviolet-sensitive gene clone 81
MutSα	Mutator S alpha
N-terminus	amino-terminus

$NaOVO_4$	sodium orthovanadate
NBS1	Nijmegen breakage syndrome 1
ND	nuclease dead
NER	nucleotide excision repair
NEFL	Neurofilament, light peptide
NF1	Neurofibromatosis type 1
NF-κB	Nuclear factor kappa B
nM	nanomolar
NP-40	nonyl phenoxypolyethoxylethanol-40
p53	Tumor protein 53
PAGE	polyacrylamide gel electrophoresis
p-H3	phospho-histone H3
PARP	poly (adenosine diphosphate-ribose) polymerase
PCR	polymerase chain reaction
PCNA	Proliferating cell nuclear antigen
PDGFRA	Platelet-derived growth factor receptor, alpha polypeptide
PI3K	Phosphoinositide 3-kinase

PMSF	phenylmethylsulfonyl fluoride
PTEN	Phosphatase and tensin homolog
PVDF	polyvinylidene fluoride
RAS	Rat sarcoma viral oncogene
RMI1/2	RecQ mediated genome instability 1/2
RPA	Replication protein A
RTEL	Regulator of telomere elongation helicase 1
rWT	siRNA-resistant wild type Exonuclease 1
SDS	sodium dodecyl sulfate
siRNA	small interfering ribonucleic acid
SLX	Structure-specific endonuclease subunit
SMC1/3	Structural maintenance of chromosomes protein 1/3
SNP	single nucleotide polymorphism
Sox2	Sex determining region Y-Box 2
SOSS1	Sensor of single-strand DNA complex subunit B1
Src	sarcoma (proto-oncogene tyrosine-protein)
STAT3	Signal transducer and activator of transcription 3

ssDNA	single-strand DNA
sWT	siRNA-sensitive wild type Exonuclease 1
TCGA	The Cancer Genome Atlas
TOPOIIIα	Topoisomerase III alpha
ug	microgram
uM	micrometer
UV	ultraviolet
VEGF	Vascular endothelial growth factor receptor
WT	wild type
XLF	X-ray repair cross-complementing protein 4-like factor
XRCC4	X-ray repair cross-complementing protein 4

CHAPTER I

GENERAL INTRODUCTION

Glioblastoma

Glioblastoma (GBM) remains the most frequently diagnosed and most deadly form of primary malignant brain cancer. Each year in the United States, physicians diagnose 10,000 new GBM cases (Dunn et al., 2012). GBMs can progress from lower-grade neoplasms, or they can arise spontaneously as Grade IV malignant GBMs. Histopathologically, grade IV GBMs are classified by the World Health Organization as having nuclear atypia, mitotic activity, pseudopalisading necrosis, microvascular proliferation, and invasion into nearby tissue (Dunn et al., 2012; Louis et al., 2007). Prior to the past decade, standard treatment for GBMs involved maximal surgical resection followed by radiotherapy given in 2 Gy fractions, 5 days per week for 6 weeks totaling 60 Gy; this strategy resulted in a 12 month median survival. Fortunately, a large-scale clinical trial testing radiation combined with concurrent and adjuvant treatment with the DNA-alkylating drug, temozolomide, extended the median survival to 14.6 months and increased the two-year overall survival from 10.4% to 26.5% (Stupp et al., 2005). However, since the approval of temozolomide, no major breakthroughs have significantly improved the outcome of GBM patients.

The lack of response to various treatment modalities is suggestive of a complex interplay of multiple signaling pathways driven by extensive genomic alterations. In an effort to define these genomic alterations, GBM was the first cancer analyzed by The Cancer Genome Atlas (TCGA). This examination of over 200 mostly primary untreated GBMs revealed the most frequently altered genes, which includes receptor tyrosine kinases (mutations or amplifications of EGFR, 45%; ERBB2, 8%; PDGFRA, 13%; and MET,4%) and tumor suppressors (mutation or deletion of PTEN, 36%; ARF, 49%; p53, 35%; and Ink4, 52%) (The Cancer Genome Atlas Research Network, 2008). In addition to distinct genomic alterations, the co-occurrence of

specific commonly altered genes has led to the identification of four GBM subtypes: classical, mesenchymal, proneural, and neural. In brief, classical GBMs exhibit PTEN loss and EGFR amplification and respond best to standard therapy. Mesenchymal tumors present with NF1 deletion and MET expression and tend to have high levels of necrosis. Further, proneural tumors exhibit PDGFRA amplification or IDH1 mutations and typically do not respond to therapy but have a better prognosis than other subtypes, and the neural subtype expresses neural markers such as NEFL and GABRA1 (Verhaak et al., 2010).

Despite a fairly strong understanding of the oncogenic alterations that comprise GBM, relatively little is known about the risk factors associated with GBM development. Currently, the only known risk factor is exposure to ionizing radiation (IR). Most of the evidence in support of this comes from pediatric patients exposed to cranial therapeutic radiation who then present with GBMs later in life (Salvati et al., 2003; Neglia et al. 2006; Calvin, et al. 1990). Therefore, we need to develop models to better understand how IR triggers gliomagenesis. Recent work from our lab using IR as a driver of gliomagenesis in Nestin-Cre mice with deletions of Ink4a, Ink4b, and Arf in the brain revealed Met amplification as the most common genetic alteration following IR exposure (Fig. 1.1) (Camacho et al., 2015). Therefore, in the work presented here, we have focused on understanding how Met amplification alters the molecular signaling and phenotypes associated with GBM.

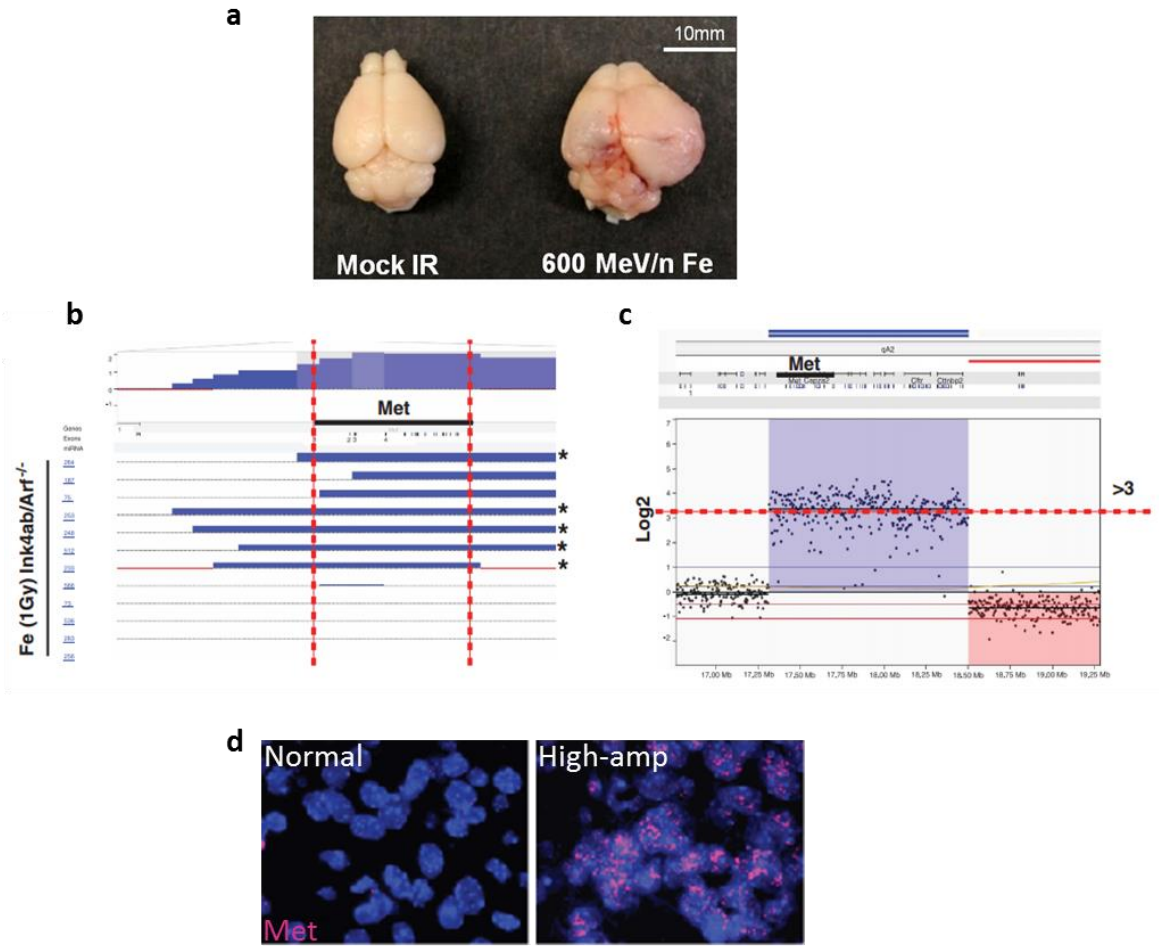

Figure 1.1. Ionizing radiation triggers gliomas with Met amplification. (a) Nestin-Cre; Ink4a/b$^{-/-}$;Arf$^{f/f}$ mice form GBMs at 2 months post-irradiation with Fe ions. (b) aCGH of 12 tumors indicating amplification of the Met locus with (c) a log2 ratio greater than 3. (d) GBMs show high Met amplification by FISH analysis compared to normal brain. (Modified from Camacho et al., 2015).

MET Receptor Tyrosine Kinase

The proto-oncogene MET is a receptor tyrosine kinase which resides on the surface of many epithelial cell types and contains a C-terminal tail, an intracellular domain with tyrosine kinase activity, a transmembrane domain, and an extracellular domain. The extracellular domain contains the binding site for the ligand of MET, the hepatocyte growth factor (HGF), which is

secreted by mesenchymal cells (Petrini, 2015). Binding of HGF to MET leads to MET homo-dimerization and activation through transphosphorylation of the Tyr1234 and Tyr1235 residues located in the cytoplasmic portion of the receptor (Koschut et al., 2016; Langati et al., 1994). Two additional tyrosines, Tyr1349 and Tyr1356, serve as docking sites for downstream signal transducers, such as growth factor receptor-bound protein 2 (Grb2), Src, phosphatidylinositol 3-kinase (PI3K), and Grb2-associated binding protein 1 (Gab1), among others (Fig. 1.2) (Ponzetto et al., 1994; Lock et al., 2003; Ponzetto et al., 1993; Gastaldi et al., 2010; Nguyen, et al 1997; Petrini et al., 2015). These proteins elicit phosphorylation-driven signal transduction cascades through multiple pathways including RAS-MAPK, PI3K-AKT, STAT3, SRC-FAK, and VEGF. Signaling through these pathways is essential for normal embryogenesis and development, in addition to tissue repair and wound healing during adulthood. However, in a cancer setting, these pathways are high-jacked to promote proliferation, anchorage-independent growth, migration and invasion, survival, and angiogenesis (Petrini et al., 2015; Skead et al., 2015). Additionally, MET signaling can be coupled with that of other receptor tyrosine kinases; this was demonstrated by Pillay et al. by showing that EGFRvIII, which is commonly expressed in GBM and activates similar downstream pathways as MET, can activate MET in an HGF-independent manner, thus indicating plasticity in receptor tyrosine kinase signaling (Pillay et al., 2009). Therefore, MET signaling can be influenced in a variety of ways and lead to various cellular phenotypes that foster tumorigenesis.

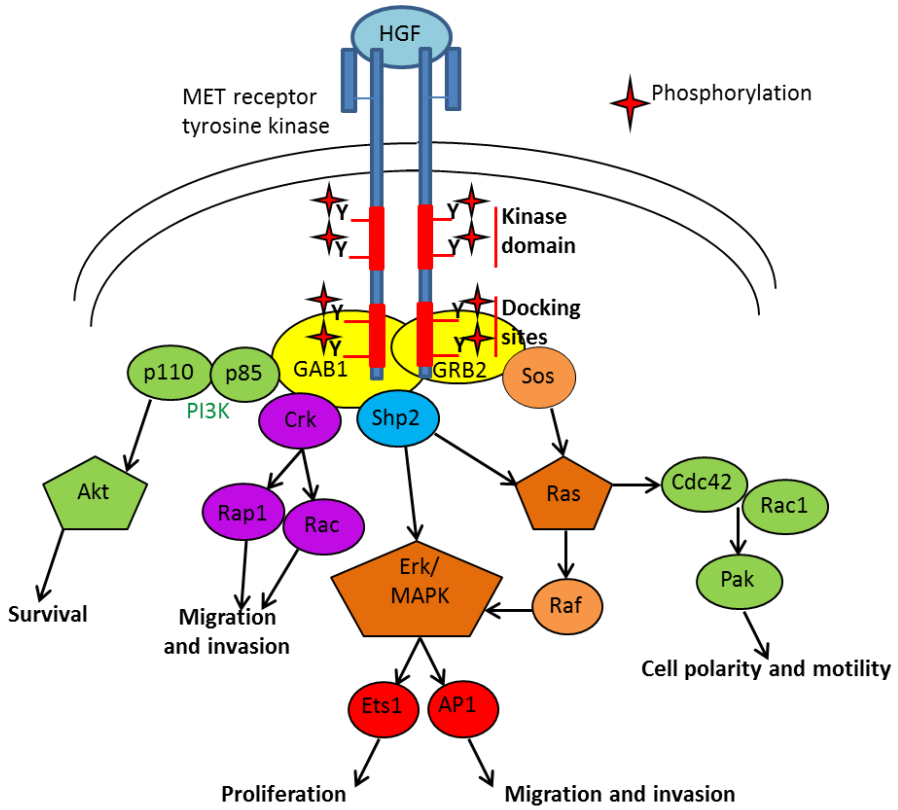

Figure 1.2. MET receptor tyrosine kinase signaling pathway. Binding of HGF to the extracellular domain of MET induces MET homo-dimerization and subsequent activation through transphosphorylation of its tyrosine kinase activation and docking site residues. These phosphorylation events promote binding of substrates including GAB1 and GRB2 which activate downstream signaling cascades resulting in proliferation, migration, and survival. (Modified from Gastaldi et al., 2010).

Numerous tumor types display MET alterations. Amplification, mutation, or over-expression of MET have all been reported in colorectal, ovarian, and non-small cell lung cancers, among others (Petrini et al., 2015; Skead et al., 2015). In the context of GBM, MET is locally amplified in about 5% of tumors, while chromosome 7q where MET, HGF, and EGFR reside is broadly amplified in nearly 20% of GBM cases (Beroukhim et al., 2007). MET mRNA transcripts and protein levels are also high in about 30% of GBMs (Xie et al., 2011; Kong et al., 2009). Importantly, MET over-expression is associated with a more invasive tumor phenotype and a worse prognosis (Kong et al., 2009). Therefore, in certain GBM patient populations, MET

signaling likely plays a fundamental role in disease progression, which warrants studies focused on understanding how MET drives aggressive phenotypes associated with GBM.

In addition to the classical roles associated with MET signaling in cancers, recent work has revealed that MET maintains the cancer stem cell phenotype in GBM. A study using GBM neurospheres found that stimulating MET with HGF caused an increase in transcription of the reprogramming transcription factors Nanog, Sox2, Myc, Klf4, and Oct4, and knockdown of Nanog prevented neurosphere formation (Li et al., 2011). The authors suggest that MET-driven expression of these reprogramming transcription factors can block differentiation of cancer stem cells, promote self-renewal, and stimulate dedifferentiation of cancer progenitor cells back to a cancer stem cell state (Li et al., 2011). Similar findings demonstrated that high MET-expressing primary GBM cells form neurospheres in stem cell media and tumors in sub-cutaneous and orthotopic transplantation models (Joo et al., 2012; De Bacco et al., 2012). Since strong evidence exists supporting MET as a promoter of the cancer stem cell phenotype, understanding how MET alters the signaling pathways of GBM cancer stem cells could aid in the development of targeted therapeutic strategies.

Glioblastoma Cancer Stem Cells

The brain is composed in a hierarchical fashion with stem cells at the top. Stem cells can both self-renew and give rise to transient amplifying cells, which form differentiated progeny that is constrained to a specific lineage. In a tumor setting, cancer stem cells are hypothesized to possess many of the same properties as normal stem cells. Functionally, this means that a cancer stem cell must be able to give rise to a tumor that mimics the cellular composition of the parental tumor (Lathia et al., 2015).

Characterizing cancer stem cells in order to understand their biology is critical for tumor treatment, as cancer stem cells can repopulate a tumor after temozolomide treatment in GBM mouse models, suggesting that the GBM stem cells are therapy resistant (Chen et al., 2012). Studies have found that GBM stem cells are radioresistant as well, and multiple mechanisms by which this resistance occurs have been proposed. For example, enhanced NF-κB signaling and EZH2-driven epigenetic modulation support radioresistance of GBM cancer stem cells (Bhat et al., 2013; Kim et al., 2015). Furthermore, Wang et al. describe how activation of the Notch pathway drives radioresistance but does not alter activation of CHK1 and CHK2, two major signaling kinases involved in the DNA damage response (Wang et al., 2009). In contrast, Ropolo et al. suggest that enhanced activation of CHK1 and CHK2 does drive radioresistance of GBM stem cells, but report no differences in base excision, single-strand break, or double-strand break repair capabilities (Ropolo et al., 2009). Still another study finds that GBM-initiating cells are therapy resistant due to enhanced PARP activity, which facilitates repair of single-strand breaks, and work by Lim et al. implicates enhanced homologous recombination repair of double-strand breaks (Venere et al., 2014; Lim et al., 2012). Therefore, numerous contrasting mechanisms exist to explain how GBM cancer stem cells promote therapy resistance. In part, these contradicting reports may be explained by the lack of consensus in the field on strategies to enrich for glioma stem cells. Despite these differences, however, it is clear that GBM stem cells are resistant to genotoxic stress, and multiple mechanisms likely explain this phenotype, some of which implicate the DNA damage response.

DNA Damage Response

Mammalian cells are constantly experiencing DNA damage and alteration. Approximately 10 double-strand breaks occur during each cell cycle, in addition to thousands of

other chemical modifications from cellular metabolic processes or exogenous sources (Haber 1999; Ciccia et al., 2010). Depending on the extent of damage, cells invoke specific DNA damage responses. This collective effort is termed the DNA damage response (DDR), and is comprised of damage sensors, mediators, and effectors that execute the particular cellular response. The extent of DNA damage will determine whether the lesion is repaired immediately or if there is a necessity for a cell cycle arrest to allow for an extended period of time for repair. Alternatively, if the damage is too extensive to be repaired properly, the cells may undergo apoptosis or necrosis.

Damage can alter the structural integrity of DNA in a variety of ways. Therefore, cells have evolved highly specific processes to confront each type of lesion. For example, base excision repair (BER) eliminates oxidized or deaminated bases and single-strand breaks. The mismatch repair (MMR) system restores mismatched bases resulting from replication or recombination errors. Additionally, nucleotide excision repair (NER) repairs DNA modified by bulky, helix-distorting lesions, such as UV-induced pyrimidine dimers. Double-strand breaks (DSB), the most lethal form of DNA damage, are primarily repaired by non-homologous end joining (NHEJ) or homologous recombination (HR) repair pathways. With such a vast assortment of damage types, thousands of proteins are involved in the repair processes and must be under strict regulation, as any one protein itself, if left unrestrained, may pose a risk to the integrity of the genome (Helleday et al., 2014, Ciccia et al., 2010).

Double-strand break repair

If DSBs are left unrepaired, the cell loses its genomic integrity which can result in cell death. Therefore, two central pathways have evolved to repair DSBs: non-homologous end

joining (NHEJ) and homologous recombination (HR) (Fig. 1.3). Since it is imperative that DSBs are repaired, NHEJ can be utilized in any phase of the cell cycle, but with the tradeoff of inducing genomic errors, such as insertions and deletions, due to direct ligation of the DNA ends. Alternatively, HR is an error-free pathway, but takes more time for repair and is restricted to S and G2 phases of the cell cycle when a homologous sister chromatid is present to serve as a template for repair. With these two pathways, the cell is equipped to repair DSBs no matter when damage strikes, albeit with potential for error.

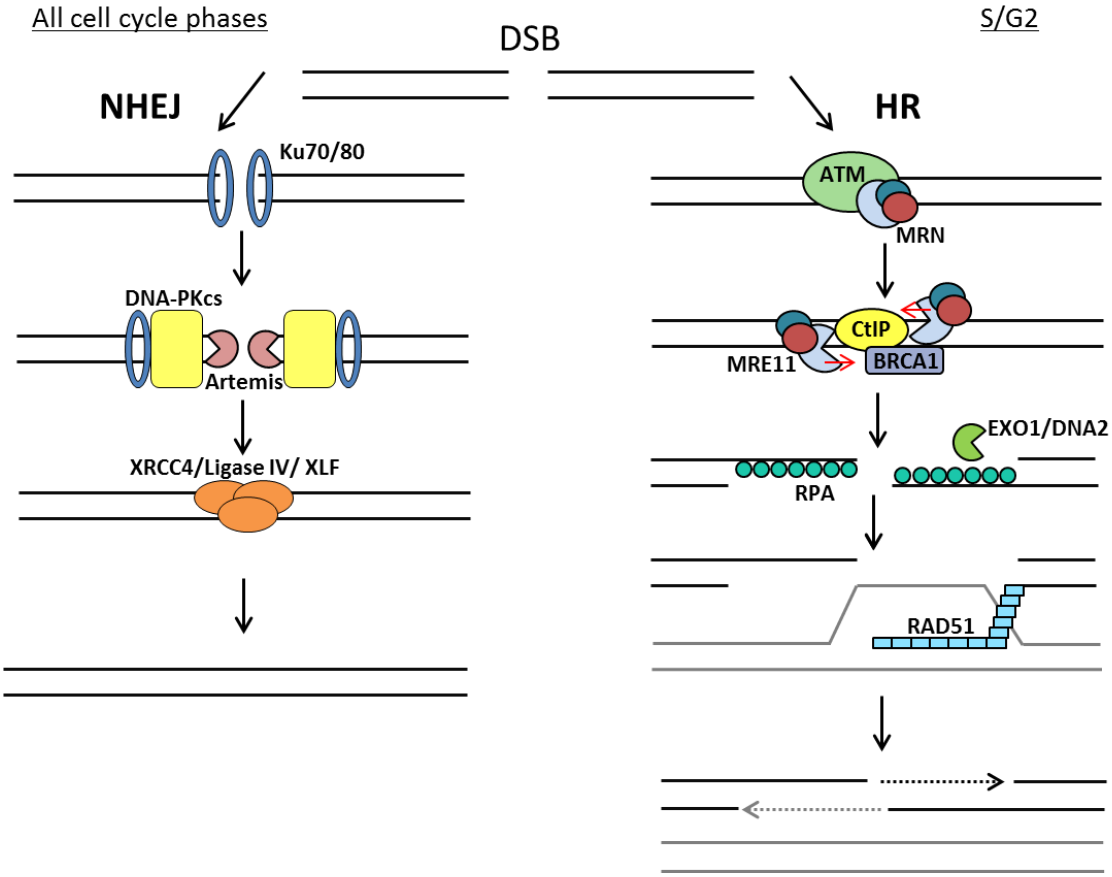

Figure 1.3. DSB repair by non-homologous end joining (NHEJ) and homologous recombination (HR). DBSs can be repaired by NHEJ in all cell cycle phases, but this pathway is error-prone since it directly ligates broken ends with minimal end-processing. HR is restrained to S/G2 phases of the cell cycle and requires resection of the DNA ends to generate a 3' overhang to search for homology within a homologous sister chromatid.

Non-homologous end joining

Upon DSB formation, the NHEJ pathway is initiated by rapid binding of the Ku70/Ku80 heterodimer around each broken DNA end to bridge them together, followed by recruitment and activation of the DNA-PK catalytic subunit (DNA-PKcs) (Hammel et al., 2010). DNA-PKcs autophosphorylates at the T2609 cluster inducing a conformational change that allows limited end-processing to ensue (Goodarzi AA et al., 2006). End-processing removes any end-blocking lesions that may prevent ligation of the DNA ends. End-processing primarily occurs by the endonuclease ARTEMIS, which directly binds to DNA-PKcs. DNA-PKcs then autophosphorylates at the S2056 cluster to restrain the end-processing step to avoid excessive resection (Ciccia et al., 2010). Following this step, XRCC4/LIG4 and XLF bind to ligate the ends (Mahaney et al., 2009). Therefore, NHEJ is a relatively simple process that can repair DSBs quickly, but the repaired DNA will likely contain insertions or deletions.

Homologous Recombination

In contrast to NHEJ, the HR DSB repair pathway perfectly restores the original DNA sequence. This error-free restoration is enabled through use of a homologous sister chromatid that serves as template during DNA synthesis, but this is limited to S and G2 phases of the cell cycle when DNA is 4N. HR is a highly complex process requiring multiple levels of regulation. During HR, the DSB is sensed by PARP and the MRN complex, which is comprised of MRE11, Rad50, and NBS1. MRE11 exhibits the endo- and exonucleolytic activity of this complex, while Rad50 bridges the DNA ends and provides ATPase activity; NBS1 directly binds to MRE11 and serves as a substrate for other proteins necessary for the nuclease activity of MRE11 (Ciccia et al., 2010). NBS1 is responsible for the recruitment of the ATM kinase, which exists as inactive

dimers that form monomers upon activation by MRN (Bakkenist et al., 2003; Lee et al., 2005; Paull 2015).

Upon break sensing and ATM activation, resection occurs to remove the 5’ strand at the break site, leaving behind a 3’ single-strand DNA (ssDNA) tail which invades the homologous sister chromatid. Resection also commits the cell to HR and prevents NHEJ from ensuing. Resection is executed in two main steps: limited resection and long-range resection (Fig. 1.4). The process of limited resection removes end-binding proteins and end-blocking lesions to allow access for the proteins that perform long-range resection. Limited resection involves a complex series of interactions between CDKs, CtIP, BRCA1, and MRN (Chen et al., 2008). CDKs phosphorylate CtIP at numerous sites to promote resection, including Thr847 and Ser327, the latter of which recruits BRCA1 to interact with and ubiquitinate CtIP to aid in localization of CtIP to the break site (Huertas et al., 2009; Yun et al., 2009; Yu et al., 2006). CDKs also phosphorylate CtIP at a cluster of 5 Ser/Thr-Pro sites which triggers CtIP to interact with NBS1 of the MRN complex (Wang et al., 2013). NBS1 is further phosphorylated by CDKs at Ser432 to promote resection (Falck et al., 2012). Together, these events permit limited resection in S and G2 phases by MRE11 which cleaves the 3’ strand at about 50-100 base pairs internal to the break, and then excises DNA towards the break, leaving behind a short 3’ overhang (Shibata et al., 2014). After this step, CtIP must be phosphorylated at Thr859 by ATM to recruit EXO1 and BLM for long-range resection (Wang et al., 2013). Long-range resection is also regulated by CDK phosphorylation of DNA2 and EXO1 exonucleases (Chen et al., 2011; Tomimatsu et al., 2014). Either EXO1 or DNA2, in complex with BLM, can execute long-range resection, which involves the excision of approximately 3000 base pairs from the 5’ strand, leaving behind a long 3’ overhang (Nimonkar et al., 2011; Zhou et al., 2014). As resection occurs, RPA and SOSS1,

both ssDNA binding proteins, compete to coat and stabilize the DNA (Myler et al., 2016). Resection must also be restrained to prevent the formation of excessively long ssDNA. To negatively regulate resection, RPA recruits the HELB translocase which inhibits EXO1 and DNA2/BLM (Tkáč et al., 2016). Furthermore, ATM phosphorylation of EXO1 at Ser714 may restrict resection by EXO1, as does an EXO1 interaction with the 14-3-3 checkpoint regulatory proteins (Bolderson et al., 2010; Chen X et al., 2015). Thus, resection must be tightly coupled to the cell cycle so that it is active only is S and G2 phases, and it must be restrained to avoid over-resection which would lead to genomic instability.

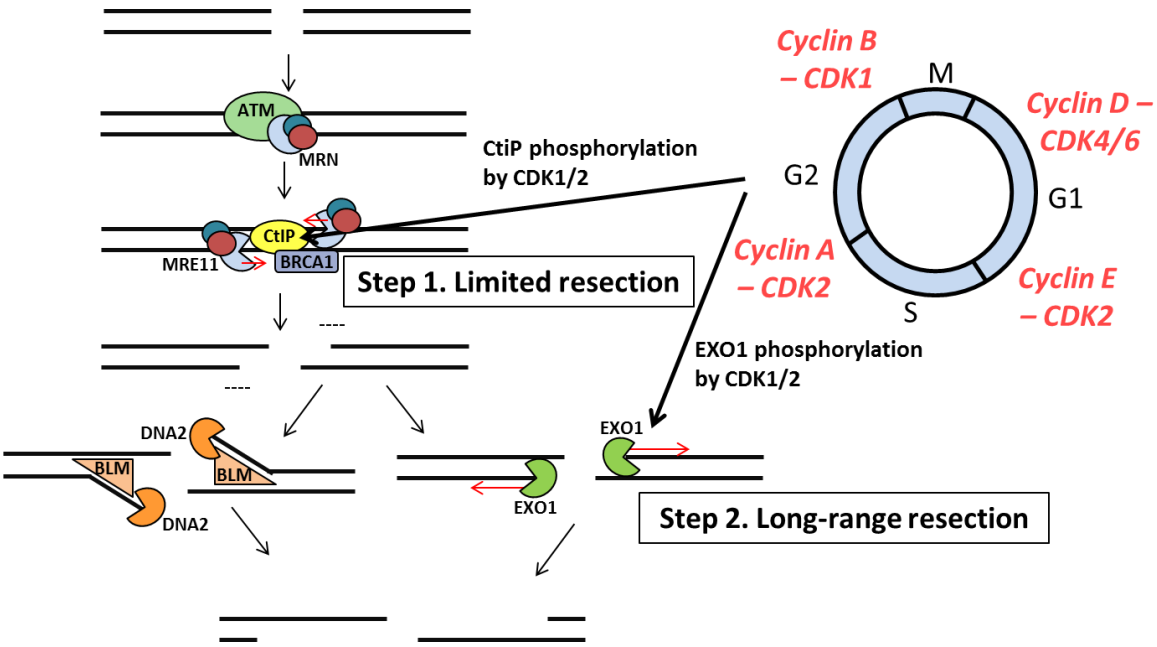

Figure 1.4. DNA-end resection is a two-step process that is coupled to S and G2 phases through CDK phosphorylation of HR proteins. Once a DSB has been sensed by MRN and ATM, CDK phosphorylation of CtIP promotes limited-resection by MRN. The second step, long-range resection, is regulated by CDK phosphorylation of DNA2 or EXO1.

After resection, the ssDNA binding proteins coating and protecting the DNA are replaced by RAD51 nucleoprotein filaments. RAD51 directly interacts with BRCA2, which facilitates the loading of RAD51 filaments onto the 3’ strand (Davies et al., 2007). RAD51 filament loading is

attenuated at the G2/M transition through CDK1 phosphorylation of BRCA2 (Esashi et al., 2005; Davies 2007). RAD51-loaded 3' DNA strands can then invade homologous sister chromatids and search for homology by forming a D-loop structure. This D-loop can either be cleaved by MUS81/EME1 to form a crossover product, or RTEL can facilitate synthesis-dependent strand annealing generating a non-crossover product (Sarbajna et al., 2014; Gwon et al., 2014; Barber et al., 2008; Ciccia et al., 2010). Another possibility is that the D-loop can result in a Holliday junction which can be resolved as a crossover or a non-crossover product mediated by GEN1 or MUS81/EME1 in complex with SLX4/SLX1 (Wyatt et al., 2013; Sarbajna et al., 2014; Matos et al., 2014). Holliday junctions can alternatively be dissolved by BLM-TOPOIIIα-RMI1-RMI2 leading to a non-crossover product (Matos et al., 2014). Having multiple processes to synthesize new DNA and properly mend the break ensures maintenance of the genome.

Exonuclease 1 (EXO1)

Resection is accepted as the key process that regulates DSB repair pathway choice by committing the cell to repair by HR. An essential enzyme that executes resection is EXO1 (Fig. 1.5). EXO1 is a member of the RAD2 nuclease family and exhibits 5' to 3' exonuclease and 5'-flap endonuclease activity (Li et al., 1999). EXO1 restores genomic stability through its functions in multiple pathways, including mismatch repair (MMR), nucleotide excision repair (NER), and HR, in addition to maintaining telomeres (Tishkoff DX et al., 1998; Giannattasio et al., 2010; Bolderson et al., 2010; Tomimatsu et al., 2012; Schaetzlein et al., 2007). In these pathways, EXO1 excises damaged and/or surrounding bases using its N-terminal nuclease domain. Its N-terminus is very well-conserved and well-ordered, which made it possible to recently crystalize this domain of EXO1 (Orans et al., 2011). The crystalized nuclease domain encompassed the first 352 residues in complex with a 10 base pair DNA duplex that mimics a

MMR intermediate substrate (Orans et al., 2011). While this N-terminal catalytic subunit is rigid in structure, the C-terminus is not well-ordered, and the sequence is divergent among family members, perhaps to accommodate numerous protein interactions (Orans et al., 2011). Indeed, the MMR-related functions of EXO1 are mediated through several C-terminal protein interactions, including MLH1, MSH2, and MSH3 (Schmutte et al., 2001). Interestingly, MLH1 binds to two regions on the C-terminus of EXO1, and in addition to its role in MMR, has also been implicated in recruiting EXO1 to DSBs (Liberti et al., 2011). Other EXO1-interacting proteins including PCNA and BRCA1 have roles in EXO1 DSB localization as well (Chen et al., 2013; Tomimatsu et al., 2014). Furthermore, BLM helicase increases the affinity of EXO1 to DNA ends (Nimonkar et al., 2008; Nimonkar et al., 2011). Although the exact choreography of these protein interactions is unclear, once EXO1 has localized to the DNA ends, it resects in a 5’ to 3’ direction to generate a 3’ DNA overhang that can be used as a substrate for homology search during HR (Li et al., 1999; Tomimatsu et al., 2012). To restrain the nucleolytic activity of EXO1 to terminate resection, multiple mechanisms exist, including phosphorylation by ATM at EXO1 Ser714, an interaction with the 14-3-3 proteins, and possibly an interaction with CtIP (Bolderson et al., 2010; Chen X et al., 2015; Eid et al., 2010). Although EXO1 interacts with a number of HR-relevant DNA repair proteins, such as BLM, CtiP, and BRCA1, the binding sites of each protein are not well-defined.

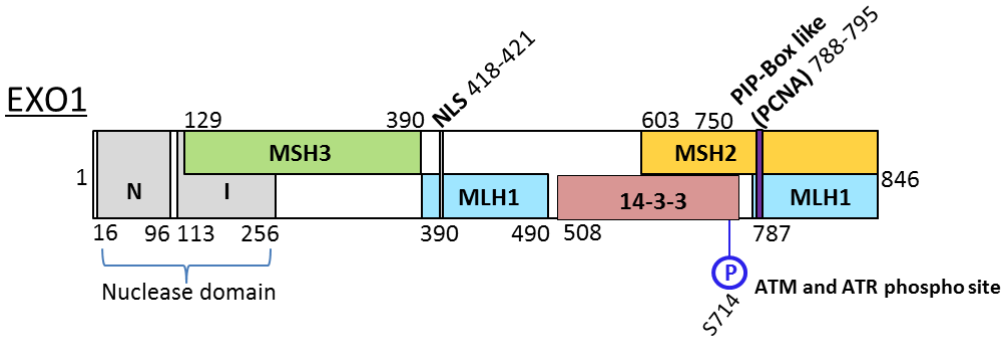

Figure 1.5. Sites and domains of EXO1. The N-terminus of EXO1 contains a well-conserved nuclease domain. The C-terminus includes binding sites and post-translational modifications for several proteins which regulate the nuclease activity of EXO1 in multiple DNA repair pathways.

Due to its fundamental role in preserving genomic integrity, alterations in EXO1 have implications in disease. Mice lacking Exo1 have a shortened lifespan, sterility due to meiotic defects, and an increase in tumor formation, specifically lymphoma (Wei et al., 2003). In humans, breast cancers often have amplification of EXO1, and this is directly linked to a decrease in survival (Muthuswami et al., 2013). Additionally, germline mutations in EXO1 may be associated with an increased risk of hereditary nonpolyposis colorectal cancer (HNPCC) and atypical HNPCC (Wu et al., 2001; Sun et al., 2002). Multiple EXO1 single nucleotide polymorphisms (SNP) have also been implicated in gastric, lung, breast, oral, and GBM cancers, but detailed studies have not examined the mechanisms which link these SNPs to carcinogenesis (Bau et al., 2009; Jin et al., 2007; Michailidou et al., 2015; Wang et al., 2009; Tsai et al., 2009; Chang et al.; 2008).

Coupling DNA repair to cell cycle checkpoints

In response to DNA DSBs, cells elicit a checkpoint response which arrests them at particular points in the cell cycle. This pause allows for the repair of damage prior to DNA

replication or cell division, which would otherwise lead to a genomically unstable state with subsequent chromosome breaks and genetic alterations. Three main DNA damage checkpoints exist: G1/S, intra-S, and G2/M. The G1/S checkpoint arrests cells in G1 to prevent damaged DNA from progressing into S phase where DNA undergoes replication, while the intra-S phase checkpoint prevents DNA synthesis and replication firing. For cells in G2 at the time of damage, G2/M checkpoint activation prevents damaged cells from entering mitosis.

The main kinases regulating cell cycle arrest are the phosphoinositide 3-kinase related kinases (PIKK), ATM and ATR. The type of damage typically dictates which kinase is activated. In the case of a DSB, ATM signaling initiates the checkpoint, but in the case of UV damage or a stalled replication fork, ATR initiates the checkpoint. In either case, ATM and ATR activate their respective checkpoint kinases, CHK2 and CHK1. Various downstream signaling events then occur depending on the particular checkpoint. In the G1/S checkpoint, CHK2 or CHK1 can phosphorylate Cdc25A, promoting its degradation. This depletion of Cdc25A causes phosphorylated CDK2-Cyclin E to accumulate in an inactive state causing a quick halt in cell cycle. This initial block is sustained by activation of p53 and subsequent accumulation of p21 which also inhibits CDK2-Cyclin E (Bartek et al., 2001; Sancar et al., 2004). In the intra-S checkpoint, the same ATM/ATR – CHK2/CHK1 – CDC25A pathway is utilized, but in order to prevent the propagation of faulty DNA, additional steps must be taken to inhibit DNA synthesis and replication firing. ATM activates BRCA1 and the MRN complex to prompt for activation of cohesins SMC1/SMC3 to inhibit DNA synthesis, and in the case of a stalled fork, ATR activation of CHK1 mediates the inhibition of Cdc7-Dbf4 to block origin firing (Yazdi et al., 2002; Sancar et al., 2004; Bartek et al., 2004; Petermann et al., 2010; Costanzo et al., 2003). In the G2/M checkpoint, CHK2 and CHK1 not only inhibit CDC25A (as described in the prior

checkpoints), but they also cause up-regulation of Wee1 to block CDK1-CyclinB from driving progression into mitosis (McGowan et al., 1995; Yarden et al., 2002).

In response to DSBs, the G2/M checkpoint is unique such that ATR activation requires ATM. Evidence has shown that the G2/M checkpoint is initiated by ATM signaling, but ATR sustains the arrest in an ATM-dependent manner. In the past it was unclear how this switch/biphasic response occurred. It is now recognized that upon sensing DSBs, ATM activates CHK2 to start the checkpoint response (Matsuoka et al., 2000; Xu et al., 2002; Kastan et al., 2000); if the break is then resected, RPA recruits ATRIP/ATR which in turn activates CHK1 to maintain the G2/M block (Liu et al., 2000; Jazayeri et al., 2005; Shiotani et al.; 2009; Shibata et al.; 2010). Work from our lab has demonstrated that EXO1-mediated resection is one switch regulating this ATM-to-ATR transition (Tomimatsu et al., 2012). Thus, EXO1-mediated resection plays a dual role by promoting HR while repressing NHEJ, and at the same time triggers ATR activation while curbing ATM activation (Fig. 1.6).

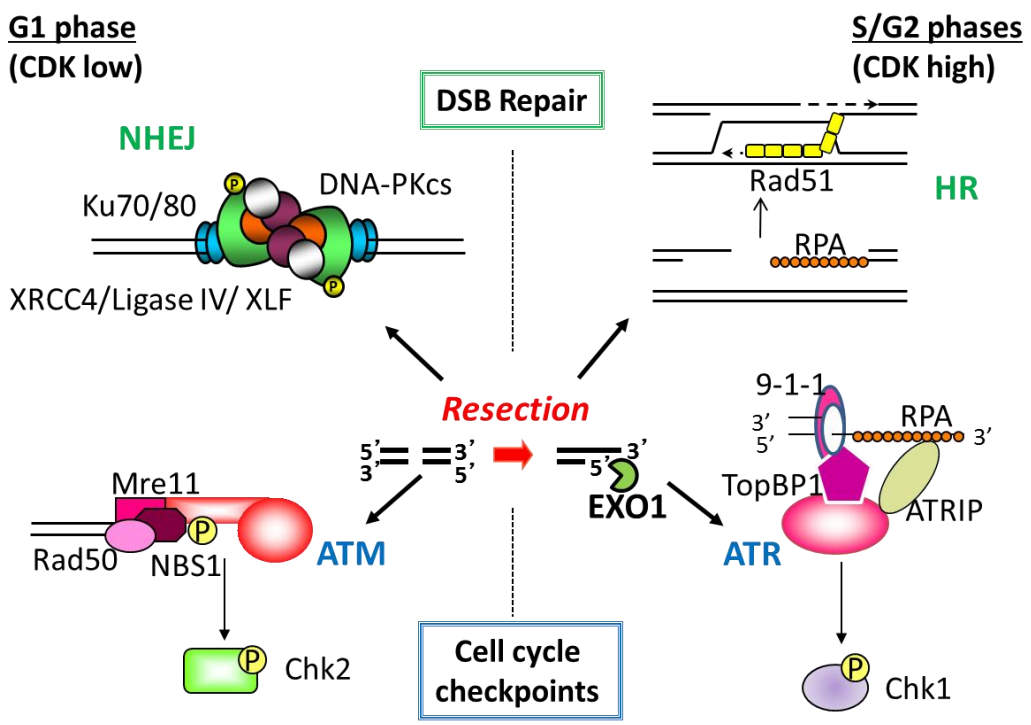

Figure 1.6. DNA-end resection by EXO1 promotes HR and a switch from ATM to ATR cell cycle checkpoint signaling. Resection dictates repair pathway choice by committing the cell to HR, thus preventing NHEJ from ensuing. In addition to repair pathway choice, resection also influences checkpoint signaling. ATM activation at DSBs initiates the G2/M checkpoint, but upon exposure of ssDNA during resection, ATM signaling is restricted, while ATR signaling is enhanced to sustain the checkpoint.

Research Summary

The research presented here aims to reveal new aspects of DNA DSB repair processes that may in the future improve the way we therapeutically target cancers. We first examined how damage-induced expression of the Met tyrosine kinase alters the DDR. We hypothesize that therapeutic resistance after treatment with DNA damaging agents is dependent on the expression of a Met-driven cancer stem cell phenotype that is characterized by an enhanced DDR. We further focused on the importance of the DDR by examining the key HR exonuclease, EXO1. We focused on assessing the roles of EXO1 domains and hypothesized that the C-terminus of EXO1 is necessary for protein interactions and post-translational modifications that facilitate a

role in both resection of DSBs during HR and checkpoint regulation. To better understand the role of EXO1 in cancer, we also investigated a cancer-associated SNP in EXO1 (N279S), which we hypothesize to alter the ability of EXO1 to resect and repair DNA. The findings of this work can be summarized as follows:

1. MET tyrosine kinase promotes a cancer stem cell phenotype, tumorigenesis, and alters the DNA damage response in glioblastoma.

2. The C-terminus of EXO1 is necessary for DSB localization, resection, and repair and serves as a platform for an interaction with BLM helicase. The C-terminus also harbors four CDK phosphorylation sites, which may play a role in modulating the duration of the G2/M checkpoint.

3. EXO1 breast cancer-associated SNP N279S exhibits both resection and DSB repair defects.

Chapter II

Role of MET amplification in altering the DNA damage response in GBM

Introduction

GBM is the most common form of primary malignant brain cancer with 10,000 newly diagnosed cases each year in the United States (Dunn et al., 2012). After diagnosis, patients undergo surgical resection, followed by treatment with ionizing radiation and temozolomide (Stupp et al., 2005). Despite aggressive treatment, these tumors invariably recur due to therapy resistance. Therefore, the median survival for these patients is a mere 15 months (Stupp et al., 2005).

With such a poor prognosis, it is crucial that we understand what triggers gliomagenesis in order to design improved therapeutic approaches. Currently, the only known risk for GBM development is exposure to ionizing radiation, but very little is known about how radiation alters the molecular signaling to promote tumorigenesis (Salvati et al., 2003; Neglia et al. 2006; Calvin, et al. 1990). In an effort to understand how radiation may initiate GBM formation, previous work from our lab utilized radiation as driver of gliomagenesis in a Nestin-Cre mouse model bearing deletions of Ink4a/b$^{-/-}$;Arf$^{f/f}$, three of the most frequently lost tumor suppressors in GBM (Camacho et al., 2015; TCGA, 2008). In this prior study, intra-cranial irradiation of Nestin-Cre;Ink4a/b$^{-/-}$;Arf$^{f/f}$ mice resulted in glioma formation approximately 50% of the time. Analysis by aCGH and FISH revealed a remarkable amplification of the Met tyrosine kinase following irradiation (Fig. 1.1) (Camacho et al., 2015).

MET is a receptor tyrosine kinase with strong clinical relevance, as MET is focally and broadly (chromosome arm 7q) amplified in approximately 5% and 19% of human GBM cases, respectively (Beroukhim et al., 2007); additionally, about 30% of glioma patients exhibit high levels of MET mRNA and protein (Xie et al., 2011; Kong et al., 2009). Clinically, high levels of

MET correlate with a decrease in median survival by approximately two months (Kong et al., 2009), suggesting that MET signaling may enhance the molecular characteristics that drive the aggressiveness of the tumor. Indeed, canonical roles of MET signaling in cancer include regulation of pathways that promote proliferation, migration, and invasion (Petrini et al., 2015; Skead et al., 2015). In addition to these established functions, MET was also recently found to maintain a GBM stem cell phenotype (Li et al., 2011; Joo et al., 2012; De Bacco et al., 2012), and new evidence suggests that GBM stem cells may contribute to the radioresistance of GBMs (Bhat et al., 2013; Kim et al., 2015; Wang et al., 2009; Ropolo et al., 2009; Venere et al., 2014; Lim et al., 2012). However, the mechanisms linking GBM cancer stem cells to therapy resistance remain disputed.

Knowing that cancer cells often have an enhanced ability to overcome DNA damage, we addressed whether Met may promote a cancer stem cell phenotype that affects the DNA damage response in GBM. As a model system, we used an ex-vivo culture generated from an Ink4a/b$^{-/-}$; Arf$^{f/f}$ radiation-induced GBM (Camacho et al., 2015). We found that Met promotes a cancer stem cell phenotype and tumorigenesis, in addition to enhancing DDR protein levels and prolonging the G2/M arrest, thus suggesting that Met may stimulate radioresistance and be a valuable target for radiosensitizing GBM.

Methods

Cell culture and drug treatments

Ink4a/b$^{-/-}$;Arf$^{f/f}$ ex-vivo cultures (Camacho et al., 2015), U87 and U51 human glioblastoma lines, and SSO4 Ink4a/Arf$^{-/-}$ murine astrocytes (a gift from Dr. Robert Bachoo) were each grown in Dulbecco's Modified Eagle Medium (DMEM) with 10% fetal bovine/newborn calf serum

mixture and 1% penicillin/streptomycin. U2OS cells were maintained in Minimal Essential Medium-alpha with 10% fetal bovine/newborn calf serum mixture and 1% penicillin/streptomycin. GBM9 neurosphere cultures (Puliyappadamba et al., 2013) were maintained in suspension in DMEM/F12 1:1 (Life Technologies) containing B27 without Vitamin A (Life Technologies), 10ng/mL epidermal growth factor (Peprotech), and 10ng/mL basic fibroblast growth factor (Peprotech). All cells were grown in 37˚C humidified incubators with 5% CO_2. To express mouse Met, human MET, and/or human HGF, we used the Gateway cloning system (Invitrogen). Mouse Met (a gift from Joan Brugge; Addgene, plasmid no. 17493) and HGF (a gift from Bob Weinberg; Addgene, plasmid no. 10901) were each originally in a pBabe-puro vector and sub-cloned into the pDONR221 vector (Invitrogen) using BP Clonase II (Invitrogen). Human MET (a gift from William Hahn; Addgene, plasmid no. 23889) was originally in pDONR223. All three genes were individually cloned into pLenti6.3/V5-DEST with LR Clonase II (Invitrogen). Virus was generated using the ViraPower Lentiviral Packaging Mix (Invitrogen). Cells were infected with virus and selected with blasticidin. For studies with Trichostatin A or 5-Azacytidine, doses of 10uM or 1uM were used, respectively, for the indicated time points.

Immunofluorescence

Cells were seeded on glass slides (Falcon) and allowed to attach overnight. Cells were fixed using 4% paraformaldehyde, permeabilized with 0.5% Triton X-100, blocked with 5% bovine serum albumin, and stained with anti-V5 (Invitrogen), anti-Sox2 (Abcam), anti-Met (Cell Signaling), or anti-53BP1 (Santa Cruz) primary antibodies and Alexa488 or Alexa568 secondary antibodies (Invitrogen).

Western blotting

Whole cell extracts were made by suspending pellets in resuspension buffer (10mM Tris (pH 6.8), 50mM NaCl, 1mM EDTA), followed by addition of 2X SDS/DTT (25% Glycerol, 0.5% SDS, 125mM Tris (pH 6.8)). Extracts were boiled, cooled, and separated via poly-acrylamide gel electrophoresis, transferred to nitrocellulose or PVDF membranes, and blotted using the following antibodies: anti-V5 (Invitrogen), anti-phospho-MET Tyr1234/1235 (Cell Signaling Technologies), anti-Sox2 (Abcam), anti-Met (Cell Signaling Technologies), anti-DNA-PK (Neomarkers), anti-ATM (GeneTex), anti-53BP1 (Santa Cruz), anti-KAP-1 (Bethyl Laboratories), anti-Chk2 (Santa Cruz), anti-Chk1 (Cell Signaling), anti-p53 (Santa Cruz), anti-Rad51 (Santa Cruz), anti-γH2AX (Millipore), anti-GAPDH (GeneTex), or anti-actin (Sigma), followed by incubation with horseradish-peroxidase-conjugated secondary antibodies against mouse or rabbit (Biorad).

Sphere formation assay

Single cells were seeded in 96-well plates in the following media: DMEM/Ham's F12 50/50 containing epidermal growth factor (20ug/mL), bFGF (25ug/mL), progesterone (20ug/mL), B-27 and insulin/transferrin-selenium supplements, doxycycline (2mg/mL), penicillin/streptomycin (50mg/mL), and fungizone antimycotic. The number of wells containing spheres was quantified and plotted.

Sub-cutaneous tumor injection

Cells were suspended in Hank's Buffered Salt Solution and either $2x10^4$, $1x10^5$, $5x10^5$, or $2.5x10^6$ cells were injected sub-cutaneously into the flanks of 6-week old Nu/Nu nude mice

(Charles River Laboratories International). Mice were monitored to determine the number of days until palpable tumors formed.

Flow cytometry for G2/M checkpoint analysis

To examine mitotic cells and cell cycle phase, cells were first irradiated with 2 Gy gamma rays using a cesium source (JL Shepherd and Associates). At the indicated time points following irradiation, cells were collected, fixed with 70% ethanol, and stored at -20˚C overnight. Cells were permeabilized with 0.25% Triton X-100 and incubated with 0.75ug anti-phospho-Histone H3 (Ser10) (Millipore) for three hours at room temperature, followed by incubation with anti-mouse Alexa488 secondary antibody. Cells were resuspended in 50ug/mL propidium iodide containing 100ug/mL RNase and analyzed using a BD CYTOMICS FC500 Flow Cytometer (Becton Dickinson).

Results

Generation of a Met-expressing GBM cell line

In our previous work, intra-cranial irradiation of Nestin-Cre mice harboring deletions of Ink4a/b$^{-/-}$;Arf$^{f/f}$ in the brain resulted in GBMs with amplification of the Met receptor tyrosine kinase gene (Fig. 1.1) (Camacho et al., 2015). We then generated ex-vivo cultures from these tumors, but although these tumors expressed Met protein initially, Met expression was rapidly lost upon growth in culture. To address this problem, we chose one line (referred to as “253 parental”) and ectopically expressed stable V5-tagged Met or β-gal (as a control) (designated as “253 Met” or “253 β-gal”, respectively) (Fig. 2.1a). We then used these cell lines to investigate the cancer stem cell properties recently associated with Met signaling (Li et al., 2011; Joo et al., 2012; De Bacco et al., 2012).

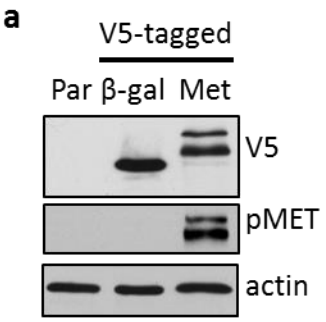

Figure 2.1. Generation of Met-expressing GBM cell line. (a) Ex-vivo culture of an Ink4a/b$^{-/-}$; Arf$^{f/f}$ murine GBM, "253 parental" (lane 1), with ectopic expression of either pLenti6.3/β-gal/V5 ("253 β-gal") (lane 2) or pLenti6.3/Met/V5 ("253 Met") (lane 3). (253 ex-vivo culture and 253 Met were generated by Camacho, CV; 253 β-gal was generated by Hardebeck, MC; Western blot was performed by Tomimatsu, N.)

Met expression promotes a cancer stem cell phenotype

To understand whether Met expression promotes a cancer stem cell phenotype, we immunofluorescence stained the 253 Met and 253 β-gal cell lines for Sox2, a reprogramming transcription factor expressed in GBM cancer stem cells (Li et al., 2011). We found that 253 Met had markedly high Sox2 levels (Fig. 2.2a), and these results were recapitulated by Western blotting (Fig. 2.2b). The 253 Met cell line could also grow as spheres when seeded as single cells in the sphere formation assay (Fig. 2.2c), suggesting that Met expression may promote self-renewal properties. To see if 253 Met cells could form tumors in-vivo, which is a characteristic of cancer stem cells, we injected various dilutions of cells sub-cutaneously into the rear flanks of nude immunocompromised mice. We found that as few as $2x10^4$ 253 Met cells were sufficient for tumor growth, while even $2.5x10^6$ 253 β-gal cells were unable to form tumors (Fig. 2.2d). These results suggest that Met expression drives a cancer stem cell phenotype and promotes tumorigenesis.

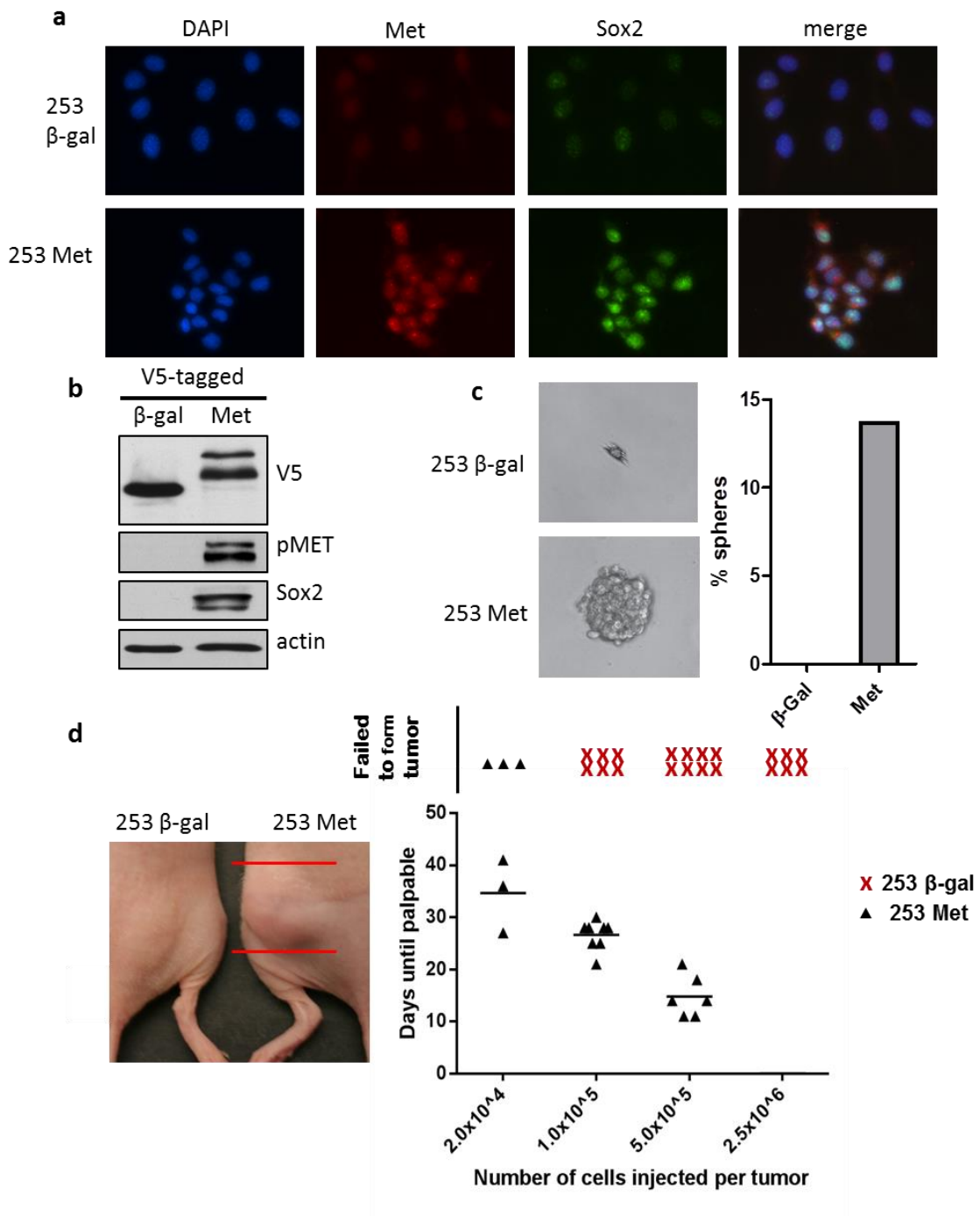

Figure 2.2. Met expression promotes a cancer stem cell phenotype. (a) 253 Met cells express Sox2 by immunofluorescence staining and (b) Western blotting (Western blot was performed by Tomimatsu, N.). (c) Sphere formation assay demonstrating that 253 Met cells seeded as single cells in stem cell media can grow as spheres. (d) Various quantities of 253 β-gal or 253 Met cells were sub-cutaneously injected into the flanks of immunocompromised mice and monitored for palpable tumors. Image taken at approximately 55 days post-injection of $1x10^5$ cells. (Modified from Camacho et al., 2015).

Met expression correlates with enhanced expression of DDR proteins

Recent evidence has suggested that GBM stem cells have an enhanced DNA damage response, although the mechanisms are unclear (Ropolo et al., 2009; Venere et al., 2014; Lim et al., 2012). Therefore, we investigated whether MET expression may influence the DNA damage response in our model system. One of the earliest responders in the DNA damage response is 53BP1, which is commonly used as a surrogate marker for DSBs (Schultz et al., 2000; Rappold et al., 2001). We found intense levels of basal 53BP1 foci in the 253 Met cell line compared to β-gal (Fig 2.3a), and this high amount of protein correlated with 53BP1 levels by Western blot (Fig 2.3b). Interestingly, under basal conditions numerous other DNA repair proteins, including Dna-pk, Atm, Kap-1, Chk2, Chk1, p53, and Rad51, expressed at significantly higher levels in the 253 Met cell line compared to β-gal (Fig 2.3b). As a control to demonstrate the high protein levels in 253 Met, we probed human U2OS cells for the same proteins and found much lower protein levels (Fig. 2.3b, lane 1). Therefore, the striking levels of DDR proteins in the 253 Met line may be indicative of a heightened capacity to respond to DNA damage.

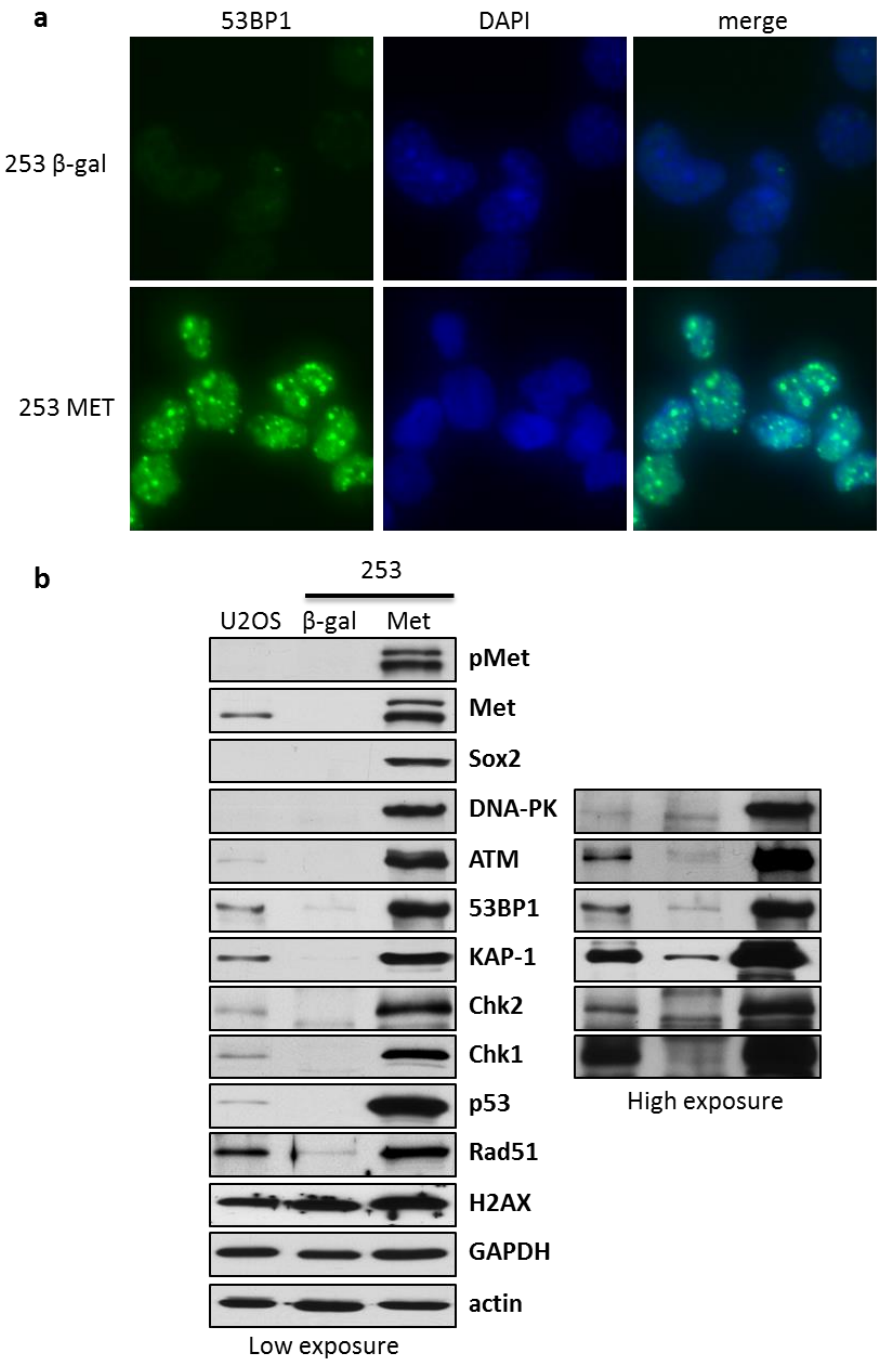

Figure 2.3. Met expression correlates with enhanced expression of DDR proteins. (a) 253 β-gal and 253 Met cells were immunofluorescence stained for 53BP1 under basal conditions. (b) Western blotting of a panel of DDR proteins expressed in U2OS (human control), 253 β-gal, and 253 Met cells. Note that the high exposure indicates the presence of DDR proteins in 253 β-gal cells, albeit at low levels. (Western blot was performed by Tomimatsu, N.)

Met expression results in a prolonged G2/M arrest

We next considered that elevated DDR proteins, many of which play essential roles in cell cycle checkpoint regulation, may translate into an altered checkpoint response after irradiation. We irradiated 253 Met and 253 β-gal cells with 2 Gy gamma rays, stained the cells for phospho-Histone H3, and performed flow-cytometry to determine the fraction of cells in mitosis. While the 253 β-gal cells recovered from the G2/M arrest in less than 8 hours after IR, the 253 Met cells had a decrease in the number of mitotic cells for up to 24 hours post-IR, suggestive of a prolonged G2/M checkpoint (Fig. 2.4). These data hint that elevated DDR proteins and a prolonged checkpoint may allow more time to faithfully repair DNA damage.

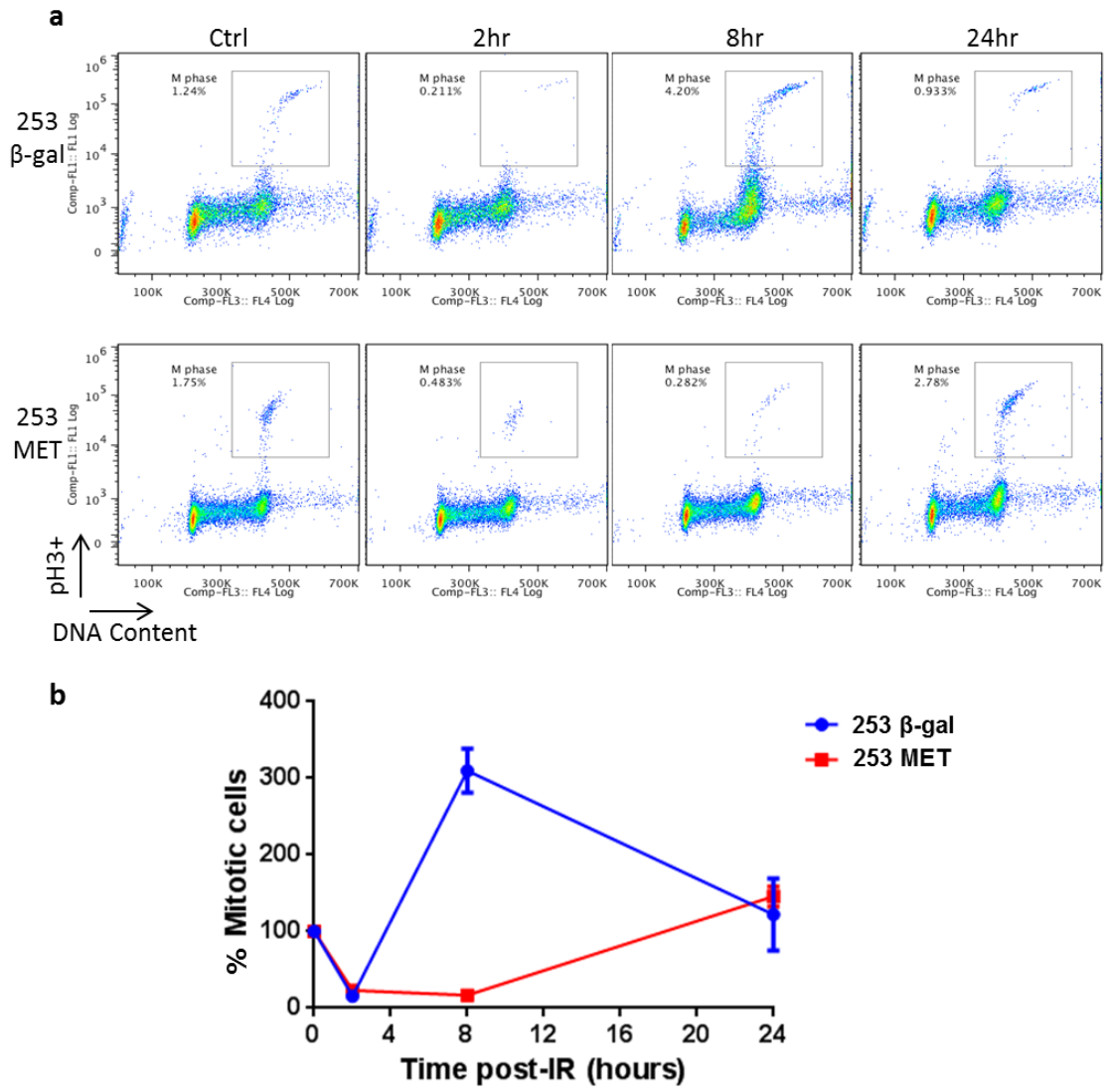

Figure 2.4. Met expression results in a prolonged G2/M arrest. (a) 253 β-gal and 253 Met cells were irradiated with 2 Gy gamma rays and stained for phospho-Histone H3 as an indicator of cells in mitosis, followed by flow cytometric analysis. (b) Quantification of phospho-Histone H3 levels.

Human GBM cells with ectopic Met/HGF expression display enhanced Sox2 levels, but eventually lose Met expression due to deacetylation

Since the 253 Met cells displayed striking cancer stem cell properties and an altered DDR, we planned to generate a human GBM tumor line with ectopic Met expression to validate our previous findings and perform future investigations. To obtain active Met, we expressed both

Met and its ligand, HGF, in the U87 human GBM cell line. At four passages after viral transduction we observed an increase in Sox2 expression (Fig. 2.5a), suggesting that in human cells Met can also drive expression of this reprogramming transcription factor. To further support this finding, we generated other Met-expressing cell lines, including the U251 human GBM line, SSO4 Ink4a/Arf$^{-/-}$ mouse astrocytes, and human GBM9 neurospheres, but unfortunately, Met expression was lost with increasing passage (Fig. 2.5b). The observed loss of Met expression can likely be explained by deacetylation of the CMV promoter (rather than promoter methylation), as treatment with the HDAC inhibitor Trichostatin A increased Met expression in SSO4 Met cells that were 9 passages post-viral transduction (Fig. 2.5c,d), while treatment with the methylation inhibitor 5-Azacytidine did not alter expression (Fig. 2.5e,f). In conclusion, despite the lack of evidence in multiple cell lines, our results suggest that Met expression promotes a cancer stem cell phenotype and alters the DNA damage response in the 253 Met cell line.

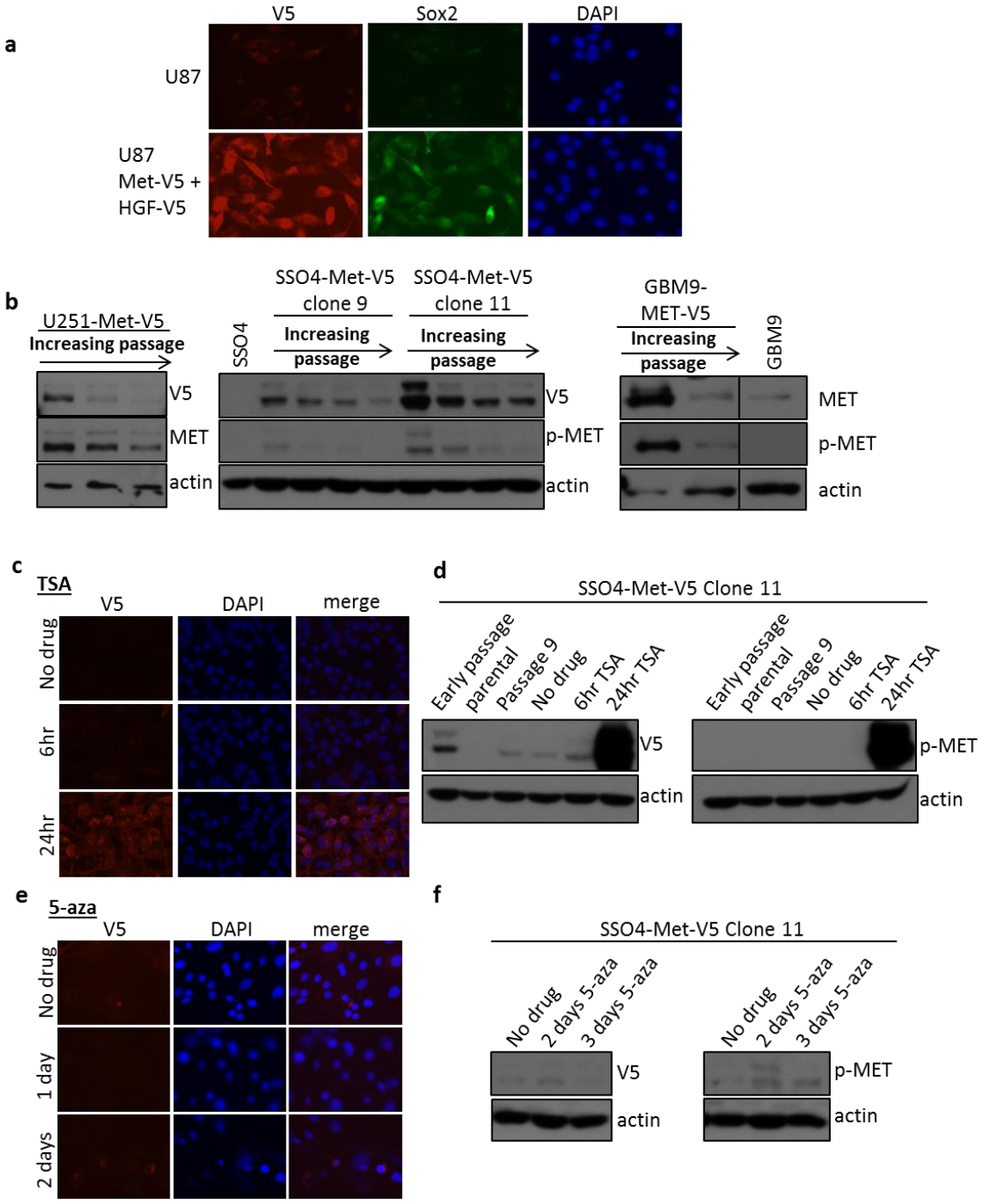

Figure 2.5. Human GBM cells with ectopic Met/HGF expression display enhanced Sox2 levels, but eventually lose Met expression due to deacetylation. (a) U87 cells expressing Met and HGF (4th passage after viral transduction) have enhanced Sox2 levels. (b) U251, SSO4, and GBM9 cell lines were all transduced with Met (mouse) or MET (human) virus, but expression was lost with increasing passage. (c,d) SSO4-Met-V5 clone 11 cells (9 passages since viral transduction) were treated with TSA or (e,f) 5-aza and examined by immunofluorescence and Western blotting.

Discussion

The current mechanisms supporting radioresistance of GBM stem cells are controversial. Some studies suggest heightened DNA repair capabilities or enhanced checkpoint activation, while others report no differences in these properties (Ropolo et al., 2009; Wang et al., 2009; Venere et al., 2014; Lim et al., 2012). Inconsistencies most likely stem from utilization of diverse model systems, such as enrichment for CD133+ cells, which is not a reliable marker, as cells without CD133 can still form tumors in mice (Joo et al., 2012). Therefore, reliable markers of GBM stem cells are necessary to allow for further investigation of the associated cancer stem cell phenotypes. In this study, we reveal how Met may be a more reliable GBM stem cell marker due to its ability to promote a GBM stem cell phenotype, and we find that MET expression significantly alters the DNA damage response.

In our model, Met is ectopically expressed in the background of Ink4a, Ink4b, and Arf deletions. These three genes are deleted in about 50% of GBM cases, thereby making our model a relevant representation of the human scenario (TCGA, 2008). Using this sensitized model, we found that Met overexpression triggers the expression of the reprogramming transcription factor, Sox2 and induces neurosphere growth in stem cell-specific media (Li et al., 2011). Moreover, Met expressing cells were capable of tumor formation in mice. These results strongly suggest that Met drives a cancer stem cell phenotype. Additionally, we found that Met expressing cells have significantly higher expression of numerous proteins involved in the DDR and have a prolonged G2/M checkpoint. We hypothesize that this longer checkpoint may allow time for error-free repair of DNA damage, and having higher baseline expression of DDR proteins may allow cells to tolerate greater levels of genomic distress.

An enhanced DDR may explain how GBM stem cells resist therapy. After a GBM patient undergoes surgical resection and receives radiation and temozolomide, both of which induce DSBs, the bulk of the tumor is destroyed. Therefore, the cancer stem cells hypothesized to repopulate the tumor must be tolerant of genomic insult and able to give rise to the other cell types comprising the tumor. Our study lends importance to this concept by providing evidence for the involvement of Met both as a driver of the cancer stem cell phenotype and a heightened DDR.

Our results corroborate other studies demonstrating that Met is an effective marker of the GBM cancer stem cell (Li et al., 2011; Joo et al., 2012; De Bacco et al., 2012), and that GBM stem cells exhibit an enhanced DDR (Ropolo et al., 2009; Venere et al., 2014; Lim et al., 2012). However, our study links these concepts by directly examining the impact of Met expression on an extensive panel of DDR proteins and correlates this with an altered checkpoint response. One caveat of our study is that the increase in DDR protein expression is not necessarily causal to the prolonged G2/M checkpoint, and outstanding questions remain, including whether increased Met expression promotes radioresistance and a heightened DNA repair capability. Additionally, it would be interesting to determine whether DSB repair pathway choice differs among Met-positive or Met-negative cells. We hypothesize that since Met expressing cells have a prolonged G2/M checkpoint, these cells may utilize the homologous recombination repair pathway, which would take longer, but would repair in an error-free manner; in contrast, we propose that the Met-negative population may slip through the G2/M checkpoint without repair or by possibly using the NHEJ pathway which is faster, but error-prone.

Although our results are restricted to a mouse GBM ex-vivo culture, we attempted to recapitulate our results in human GBM lines. We did observe an increase in Sox2 protein levels

upon expression of Met and HGF, but Met expression dropped with increasing passage most likely due to deacetylation of the CMV promoter. Therefore, we propose the use of a different promoter, such as the EF1-alpha promoter, which has been demonstrated to drive stable expression more effectively than the CMV promoter (Teschendorf et al., 2002; Qin et al., 2010). Alternatively, Met knock-in cells or neurospheres with high levels of endogenous MET could be utilized to address similar questions in a human model system.

Overall, we have demonstrated that Met expression promotes a GBM cancer stem cell phenotype through expression of Sox2, triggers tumorigenesis in mice, causes upregulation of DDR proteins, and induces a prolonged G2/M checkpoint. In the future, we must examine whether these characteristics promote radioresistance of GBM stem cells. If so, GBM patients who express high levels of MET may benefit from MET inhibitor therapy combined with standard of care treatment to radiosensitize their tumors.

Chapter III

Characterization of EXO1 sites and domains and their effects on the DNA damage response

Introduction

DNA DSBs are the most detrimental form of DNA damage. If not properly repaired, DSBs can lead to genomic instability, a hallmark of cancer (Hanahan et al., 2011). Therefore, cells have evolved two primary DSB repair pathways, non-homologous end joining (NHEJ) and homologous recombination (HR). NHEJ is active in all phases of the cell cycle but is prone to generating insertions and deletions; in contrast, HR is restricted to S and G2 phases of the cell cycle when a homologous sister chromatid is available to serve as a template for error-free repair.

The choice between these two pathways is crucial for the preservation of the genome. Recent evidence has established that repair pathway choice is regulated by an eloquent coupling of cell cycle machinery with DNA end resection, the generation of 3' ssDNA overhangs at the break site. Specifically, CDKs phosphorylate CtIP and NBS1 to regulate the first step of resection, 'limited resection', during which about 50-100 bases are removed from the 5'-ends (Huertas et al., 2009; Yun et al., 2009; Wang et al., 2013; Falck et al., 2012). An exciting study from our laboratory also recently discovered that the second step in resection, 'long-range resection', is restricted to S and G2 cell cycle phases through CDK phosphorylation of EXO1 (Tomimatsu et al., 2014). We demonstrated that CDK phosphorylation of EXO1 promotes an interaction with BRCA1 to stimulate HR and suppress NHEJ (Tomimatsu et al., 2014). However, other protein interactions regulating the function of EXO1 in HR remain to be elucidated.

In addition to resection influencing DSB repair pathway choice, resection also regulates cell cycle checkpoint signaling in response to DSBs. Once a DSB break is sensed, ATM is

recruited and phosphorylates CHK2, which initiates the G2/M checkpoint arrest (Matsuoka et al., 2000; Xu et al., 2002; Kastan et al., 2000). However, if the DSB is resected, the exposed DNA is coated by RPA which recruits ATRIP-ATR; ATR then phosphorylates CHK1, which leads to maintenance of the G2/M arrest (Liu et al., 2000; Jazayeri et al., 2005; Shiotani et al.; 2009; Shibata et al.; 2010; Tomimatsu et al., 2012). Knowing that resection is critical for this change in checkpoint signaling, we hypothesized that CDK phosphorylation of EXO1 modulates the switch between ATM and ATR activation in addition to the duration of time that cells spend in the G2/M block.

In this study, we investigated two aspects of EXO1: 1) Identifying the function of individual domains and protein interactions on EXO1 that are necessary for resection of DSBs, and 2) mapping CDK phosphorylation sites on EXO1 and asking how CDK phosphorylation of EXO1 regulates the G2/M checkpoint. We find that the C-terminus of EXO1 is required for resection and repair of DSBs because when deleted, EXO1 cannot localize to the break site. Furthermore, we find that the C-terminus of EXO1 mediates an interaction with the BLM helicase and contains four CDK phosphorylation sites. Based on preliminary results with an EXO1 knock-out model, we postulate that mutation of CDK phosphorylation sites on EXO1 will promote a premature release from the G2/M checkpoint. These findings shed new light on the complexity of EXO1's structure-function relationship.

Methods

Cell culture

HEK-293 cells were grown in Dulbecco's Modified Eagle Medium (DMEM) with 10% fetal bovine serum and 1% penicillin/streptomycin. U2OS cells were maintained in Minimal Essential

Medium-alpha with 10% fetal bovine/newborn calf serum mixture and 1% penicillin/streptomycin, and 4ug/mL puromycin was added for selection after CRISPR/Cas9 transfections. 1BR cells were grown in Minimal Essential Medium-alpha with 10% fetal bovine and 1% penicillin/streptomycin, and 1ug/mL puromycin was added for selection after CRISPR/Cas9 transfections. All cells were grown in 37˚C humidified incubators with 5% CO_2.

Cell cycle synchronization

To synchronize in late G2 phase prior to immunoprecipitation, HEK-293 cells were treated with nocodazole (100ng/mL) (Sigma) for 16 hours (Tomimatsu et al., 2014).

Mutagenesis and deletion construct generation

EXO1b was transferred from Flag2-EXO1 (Bolderson et al., 2010) into pDONR221 (Invitrogen) using BP Clonase II (Invitrogen). For mutagenesis, pDONR221/EXO1 was used as a template using the QuikChange II XL Site-Directed Mutagenesis (Stratagene), followed by an LR Clonase II enzyme (Invitrogen) reaction for transfer into the pLenti6.3/V5-DEST vector. For deletion construct generation, we performed nested/overlap extension PCRs using pDONR221/EXO1 as a template and the PrimeSTAR DNA polymerase kit (TaKaRa). Each amplified fragment was purified using the Qiagen PCR purification kit, followed by gel-purification with the QIAquick Gel Extraction kit (Qiagen). The resulting product was then transferred into pDONR221 (Invitrogen) using BP Clonase II (Invitrogen), and then cloned into the pLenti6.3/V5-DEST vector using the LR Clonase II enzyme (Invitrogen). See Appendix for primer sequences.

Transient transfections

Transient knockdown of EXO1 was performed using siRNA (siEXO #1 in Appendix) that was electroporated (Lonza) into U2OS cells. Approximately 24 hours later, cells were transfected

using Lipfectamine2000 (Invitrogen) with the indicated pLenti6.3/EXO1/V5 constructs and allowed to incubate for approximately 24 hours before the start of a particular assay. For knockdown of EXO1 in U2OS cells as a control for the CRISPR/Cas9 study, three EXO1 siRNAs were electroporated (Lonza), and on the following day, the three siRNAs were transfected using Lipofectamine2000 (Invitrogen). Cells were harvested 72 hours after the electroporation. (See Appendix for siRNA sequences).

DSB repair kinetics

Cells were seeded on glass 4-chamber slides (Falcon). For 53BP1 staining, U2OS cells were treated with 100nM CPT for 4 hours. CPT-containing media was removed and replaced with fresh media (no CPT). Cells were fixed at the indicated times using 4% paraformaldehyde. Cells were then permeabilized using 0.5% Triton X-100, blocked with 5% bovine serum albumin, and co-stained with anti-V5 (Invitrogen) and anti-53BP1 (Santa Cruz) antibodies. Cells were imaged using a Carl Zeiss Axio Imager.M2 fluorescence microscope with 40X magnification and displayed using AxioVision Rel. SE64 4.8 software. The number of V5+ cells (or V5- cells for siRNA-sensitive WT EXO1) was scored which contained 53BP1 foci greater than the average number of 53BP1 foci in the mock sample. At least 50 cells were quantified for each sample.

Resection assay

Cells were seeded onto glass 4-chamber slides (Falcon) and were irradiated with 6 Gy gamma rays using a cesium source (JL Shepherd and Associates). Three hours after IR, cells were subjected to in situ fractionation (to improve RPA foci visualization) by incubating cells on ice for 10 minutes in Extraction Buffer 1 (10mM PIPES, 100mM NaCl, 300mM sucrose, 3mM MgCl2, 1mM EGTA, and 0.5% Triton X-100), followed by a 10 minute incubation in Extraction

Buffer 2 (10mM Tris (pH 7.5), 10mM NaCl, 3mM MgCl2, 1% Tween-40, and 0.5% sodium deoxycholate). Cells were then fixed using 4% paraformaldehyde and permeabilized in 0.5% Triton X-100. Cells were blocked with 5% bovine serum albumin and stained with anti-RPA (Calbiochem). Cells were imaged using a Carl Zeiss Axio Imager.M2 fluorescence microscope and displayed using AxioVision Rel. SE64 4.8 software. Foci were quantified by counting the average number of RPA foci per nucleus and subtracting background for at least 50 cells per sample.

DSB localization using micro-laser irradiation

Cells were seeded onto poly-L-lysine-coated glass coverslips and sensitized with 10ug/mL BrdU overnight. Cells were then micro-irradiated using a pulsed nitrogen laser (Spectra-Physics; 365 nm, 10 Hz; 80% output). Five minutes after irradiation, cells were fixed with 4% paraformaldehyde and permeabilized in 0.5% Triton X-100. Cells were then blocked with 5% bovine serum albumin and co-stained with anti-V5 (Invitrogen) and anti-53BP1 (Santa Cruz) antibodies. Cells were imaged using a Carl Zeiss Axio Imager.M2 fluorescence microscope and displayed using AxioVision Rel. SE64 4.8 software.

Immunoprecipitation and Western blotting of whole-cell extracts

HEK-293 cells expressing V5-tagged EXO1 constructs were treated with 10uM MG132 for 5 hours, and in the final hour, 1uM CPT was added. Frozen cell pellets were suspended in lysis buffer (20mM Tris-HCl (pH 7.5), 80mM NaCl, 2mM EDTA, 10% glycerol, 0.2% NP-40, protease inhibitor (Sigma), and phosphatase inhibitor (Sigma), 20mM NaF, 2mM $NaOVO_4$, 20mM β-glycerophosphate, 1mM DTT, and 1mM PMSF). Mouse IgG (Santa Cruz) antibody or anti-V5 (Invitrogen) antibody were bound to M-280 sheep anti-mouse IgG Dynabeads (Life

Technologies) and incubated with cell lysate for 4 hours. Beads were washed four times with lysis buffer (20mM Tris-HCl (pH 7.5), 80mM NaCl, 2mM EDTA, 10% glycerol, 0.2% NP-40) and boiled in 1X SDS loading buffer for separation via PAGE followed by transfer onto PVDF. Membranes were blotted using anti-V5 (Invitrogen), anti-BLM (Bethyl Laboratories), anti-phospho-Threonine CDK substrate (Cell Signaling Technologies), and phospho-Serine CDK substrate (Cell Signaling Technologies) primary antibodies and horseradish peroxidase-conjugated secondary antibodies (Biorad).

CRISPR/Cas9 knock-out cell generation and PCR validation

To generate EXO1 knock-outs, U2OS and 1BR cells were transfected using Lipofectamine2000 (Invitrogen) with human Cas9, a donor vector containing a puromycin resistance gene, and a gRNA (PCMV-spCas9-T2A-mKate-U6-sgRNA) targeting exon 3 of EXO1. To generate AAVS1 knock-outs, U2OS and 1BR cells were transfected using Lipofectamine2000 with a plasmid encoding for both Cas9 and the gRNA (PCMV-Cas9-t2a-mkate-U6-gRNA), in addition to a donor vector containing a puromycin resistance gene. (All of these plasmids were kindly donated by Dr. Leonidis Bleris, University of Texas at Dallas. See Appendix for gRNA target sequences). The transfected cells were maintained in 4ug/mL (U2OS) or 1ug/mL (1BR) puromycin for selection. Single cell clones were grown and screened by PCR for insertion of the puromycin resistance gene. Primers were designed to bind regions flanking the puromycin gene (see Appendix for primer sequences) to distinguish between an intact parental locus or the puromycin insertion. PCR was carried out using the PrimeSTAR DNA polymerase kit (TaKaRa).

Nuclear extraction and Western blotting

Nuclear extracts were generated from U2OS and 1BR cell lines to blot for endogenous EXO1 by resuspending the pellets in hypotonic lysis buffer (10mM Tris-HCl (pH 7.5), 1.5mM $MgCl_2$, 5mM KCl, protease inhibitor (Sigma), and phosphatase inhibitor (Sigma), 20mM NaF, 2mM $NaOVO_4$, 20mM β-glycerophosphate, 1mM DTT, and 1mM PMSF). The mixture was spun down and the resultant pellet was resuspended in nuclear extraction buffer (50mM Tris-HCl (pH 7.5), 0.5M NaCl, 2mM EDTA, 10% sucrose, 10% glycerol, protease inhibitor (Sigma), and phosphatase inhibitor (Sigma), 20mM NaF, 2mM $NaOVO_4$, 20mM β-glycerophosphate, 1mM DTT, and 1mM PMSF). Nuclear extracts were mixed with 2X SDS loading buffer and boiled. Extracts were separated via PAGE followed by transfer onto PVDF. Membranes were blotted using anti-EXO1 (Bethyl Laboratories) and anti-β-actin (Santa Cruz) primary antibodies and horseradish peroxidase-conjugated secondary antibodies (Biorad).

Flow cytometry for G2/M checkpoint analysis

For cell cycle analysis, cells were irradiated with 4 Gy gamma rays using a cesium source (JL Shepherd and Associates). At the indicated time points following irradiation, cells were collected, fixed with 70% ethanol, and stored at -20˚C overnight. Cells were permeabilized with 0.25% Triton X-100 and incubated with 0.75ug anti-phospho-Histone H3 (Ser10) (Millipore) for three hours at room temperature, followed by incubation with anti-mouse Alexa488 secondary antibody. Cells were resuspended in 50ug/mL propidium iodide with 100ug/mL RNase and analyzed using a Becton Dickinson FACSCalibur flow cytometer. Data was acquired using CellQuest Pro and analyzed on FlowJo software.

Results

The C-terminus of EXO1 is necessary for DSB resection and repair

To investigate domains on EXO1 necessary for DSB repair, we generated a panel of V5-tagged EXO1 deletion constructs spanning the length of the gene (Fig. 3.1a,b). We then generated a model system in which we knocked down endogenous EXO1 using siRNA and expressed siRNA-sensitive WT EXO1 (sWT; negative control), siRNA-resistant WT EXO1 (rWT; positive control), or siRNA-resistant EXO1 deletion constructs (Fig. 3.1c). One particular construct, d353-846, which contains the nuclease domain and lacks the C-terminus, exhibits a resection defect indicated by a lack of RPA foci after irradiation compared to rWT EXO1 (Fig. 3.1d). Consequently, this construct also has a severe DSB repair defect following CPT treatment (Fig. 3.1e). These results indicate that the C-terminus of EXO1 is necessary for regulating the function of the nuclease domain in DSB repair.

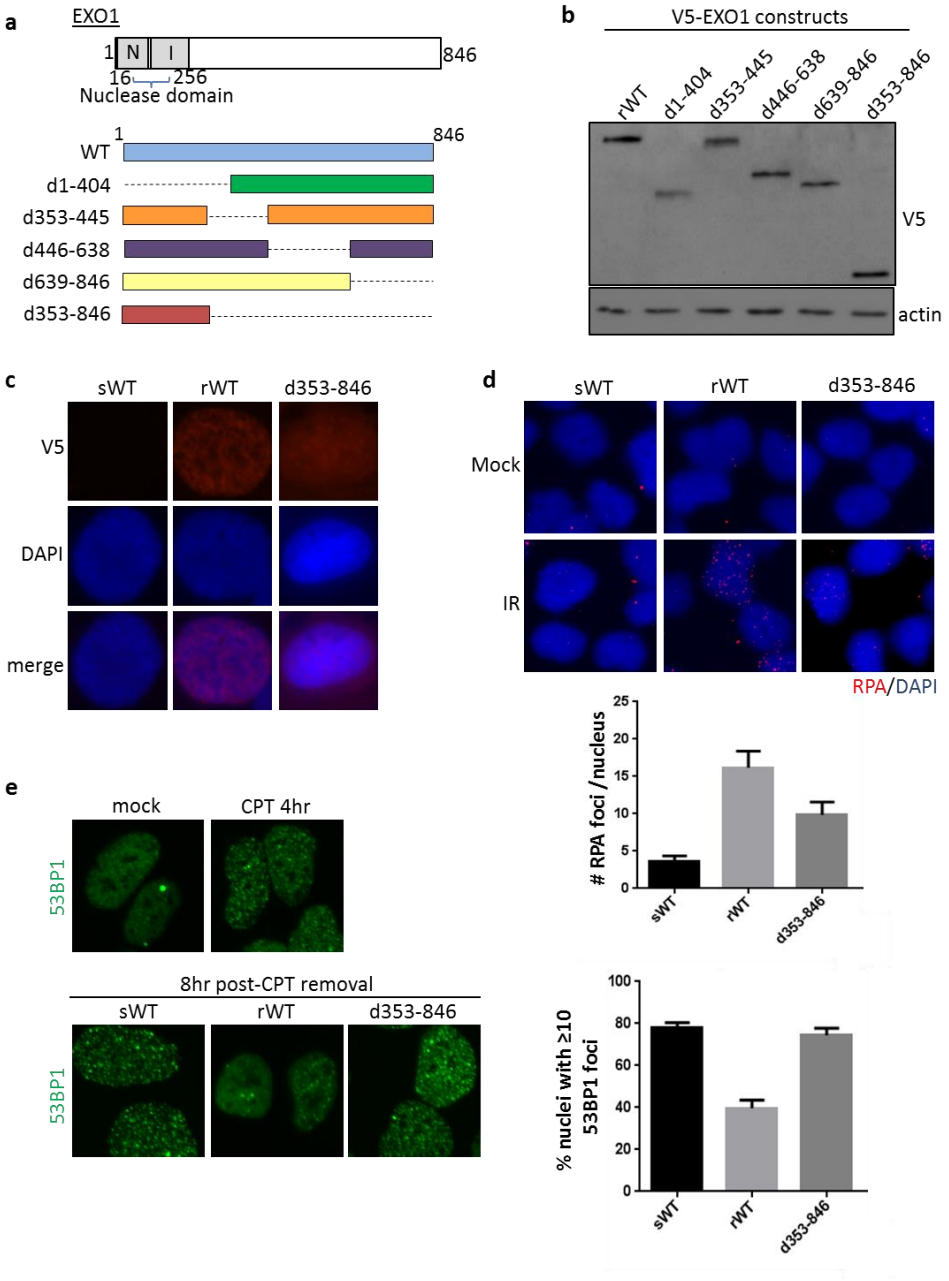

Figure 3.1. The C-terminus of EXO1 is necessary for DSB resection and repair. (a) Schematic of deletion constructs spanning the EXO1 gene. (b) Western blot HEK-293 cells expressing V5-tagged EXO1 deletion constructs. (c) Model system showing U2OS cells with knockdown of EXO1 by siRNA and complementation with V5-tagged siRNA-sensitive EXO1 (sWT), siRNA-resistant EXO1 (rWT), or siRNA-resistant EXO1 d353-846. (d) U2OS cells with knockdown of EXO1 and expression of the indicated constructs were irradiated and immunofluorescence stained for RPA foci. (e) U2OS cells with knockdown of EXO1 and expression of the indicated constructs were treated with CPT and immunofluorescence stained for 53BP1.

DSB localization of EXO1 requires its C-terminus

We next hypothesized that the resection defect we observed may be caused by an inability of EXO1 to localize to the break site without its C-terminus. To determine whether EXO1 d353-846 could localize to the site of DSBs, we used micro-laser irradiation to generate a line of damage across the nuclei, followed by immunofluorescence co-staining of 53BP1 and V5. Interestingly, EXO1 d353-846 was unable to co-localize with 53BP1, suggesting that the nuclease domain alone is insufficient for localizing to a break site (Fig. 3.2). On the other hand, a deletion construct containing only the C-terminus (EXO1 d1-404) was able to localize to the break site as previously reported (Fig. 3.2) (Liberti et al., 2011). This result led us to hypothesize that proteins may interact with the C-terminus to promote its localization to DSB sites.

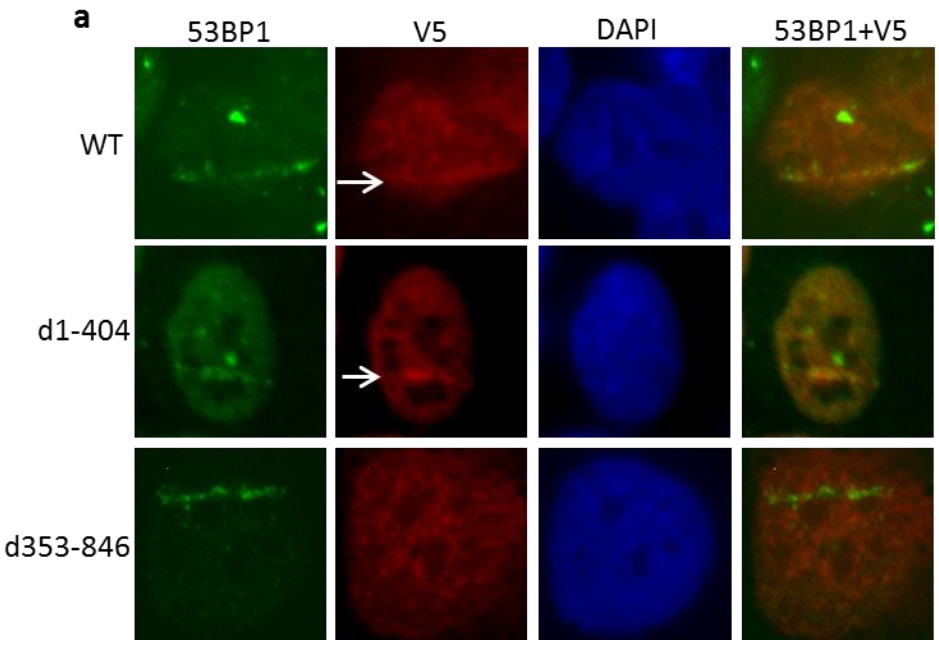

Figure 3.2. DSB localization of EXO1 requires its C-terminus. (a) U2OS cells with siRNA knockdown of endogenous EXO1 and expression of V5-tagged EXO1 constructs were co-immunofluorescence stained for 53BP1 and V5 five minutes following micro-laser irradiation. Arrows indicate V5 accumulation.

BLM helicase interacts with the C-terminus of EXO1

Knowing that EXO1 and BLM interact to increase EXO1's affinity for DNA ends (Nimonkar et al., 2008; Nimonkar et al., 2011), we examined whether BLM may differentially interact with the N- and C-termini of EXO1. We found that under stabilizing and damage-inducing conditions, the C-terminus of EXO1 (d1-404) interacts with BLM, and this interaction is weakened with EXO1 WT and EXO1 d353-846 (nuclease domain) (Fig. 3.3), suggesting that the C-terminus may serve as a platform for BLM and perhaps other proteins which may regulate the function of EXO1 during DSB repair.

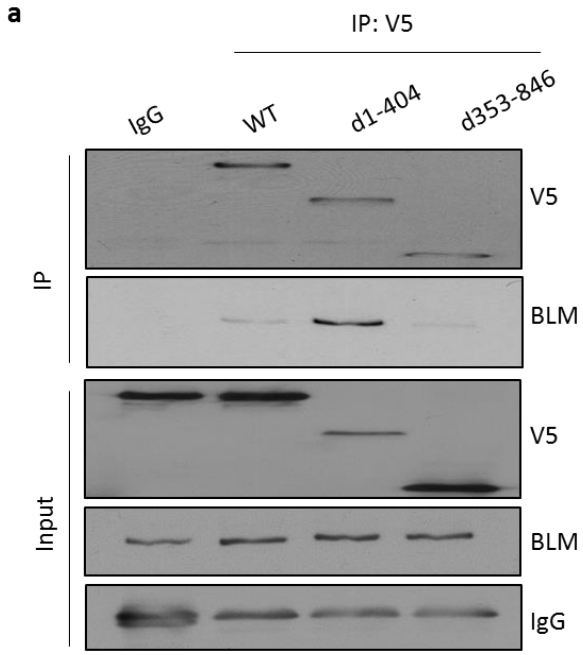

Figure 3.3. BLM helicase interacts with the C-terminus of EXO1. (a) HEK-293 cells expressing V5-tagged EXO1 constructs were treated with MG132 and CPT. Whole cell extracts were co-immunoprecipitated using V5 antibody and probed by Western blot using the specified antibodies.

EXO1 harbors four C-terminal CDK phosphorylation sites that are necessary for resection

In addition to mapping a C-terminal protein interaction, we also asked if there are post-translational modifications on the C-terminus of EXO1 which may regulate its activity. Since recent results from our lab demonstrated that EXO1 is phosphorylated by CDK1 and CDK2 in S and G2 phases of the cell cycle, we performed site-directed mutagenesis to identify the sites on EXO1 that are phosphorylated by CDKs. CDKs phosphorylate at Ser/Thr-Pro consensus sites, and EXO1 contains ten such sites (Fig. 3.4a). We knocked down endogenous EXO1, complemented the cells with siRNA-sensitive WT EXO1 or siRNA-resistant WT EXO1 which was then mutated at each of the ten putative CDK consensus sites, and screened for RPA foci after IR (Fig. 3.4b). We found that mutation of the last four Ser-Thr/Pro sites (S639A, T732A, S815A, T824A; signified as ‘4A-EXO1’) on the C-terminus abrogated resection (Fig. 3.4c). Importantly, mutation of the CDK sites abolished phosphorylation of EXO1 when probed with phospho-serine- or phospho-threonine-CDK substrate antibodies. (Fig. 3.4d). Therefore, CDK phosphorylation of EXO1 on four C-terminal sites is essential for EXO1-mediated resection (Tomimatsu et al., 2014).

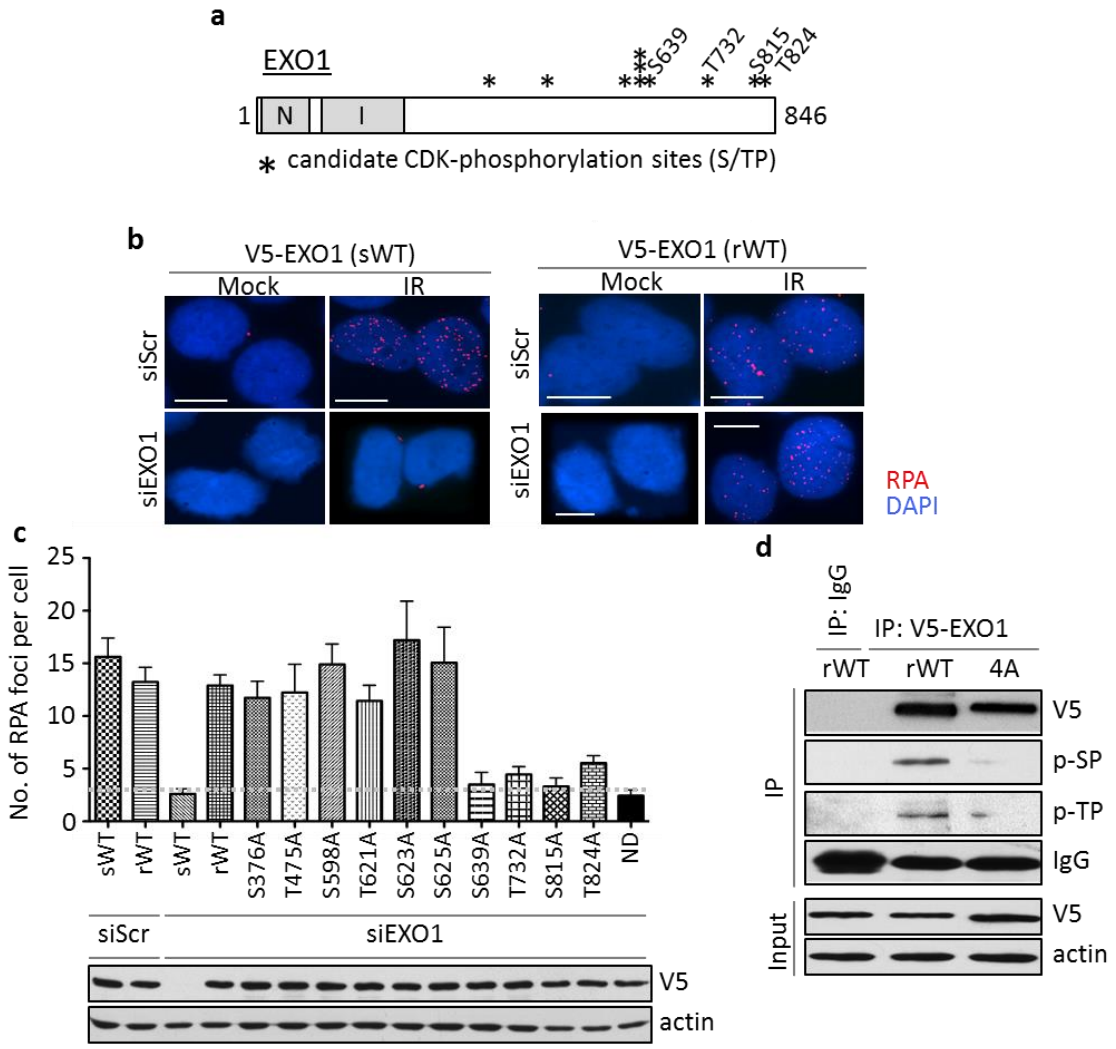

Figure 3.4. EXO1 harbors four C-terminal CDK phosphorylation sites that are necessary for resection. (a) EXO1 schematic showing putative CDK phosphorylation consensus sites (Ser/Thr-Pro). (b) U2OS cells with scrambled siRNA or siRNA against EXO1 were complemented with V5-tagged siRNA-sensitive WT EXO1 (sWT) or siRNA-resistant WT EXO1 (rWT), irradiated, and immunofluorescence stained for RPA. (c) U2OS cells with knockdown of endogenous EXO1 and complemented with V5-tagged siRNA-resistant EXO1 that is individually mutated at the indicated Ser/Thr-Pro sites were irradiated and immunofluorescence stained for RPA to analyze resection defects. All mutants expressed at similar levels as indicated by the V5 Western blot. (d) HEK-293 cells expressing V5-tagged rWT- or 4A-EXO1 (4A signifies the following mutations: S639A, T732A, S815A, T824A) were synchronized in G2, immunoprecipitated for V5, and immunoblotted using the indicated antibodies to examine phosphorylation of EXO1. (All assays were performed by Tomimatsu, N. Hardebeck, MC contributed to the site-directed mutagenesis.) (Modified from Tomimatsu et al., 2014).

Generation of EXO1 knock-out cells for checkpoint analysis

Since CDK phosphorylation of EXO1 promotes resection and HR (Tomimatsu et al., 2014) and resection requires a halt in the cell cycle, we asked how CDK phosphorylation of EXO1 may influence the order of activation of the ATM and ATR kinases and the duration of the G2/M checkpoint. Since checkpoint studies require long time points, we used CRISPR/Cas9 technology to generate EXO1 knock-out cell lines which could then be complemented with 4A-EXO1. The CRISPR/Cas9-mediated HR strategy targets exon 3 of EXO1, which encodes for a portion of the nuclease domain, and inserts a puromycin resistance gene with a stop codon resulting in early termination of transcription and a knock-out phenotype (Fig. 3.5a). The same strategy was implemented to generate control cells by targeting the AAVS1 safe harbor locus.

We first attempted to generate knock-out cell lines using U2OS osteosarcoma cells. We screened clones using a PCR strategy in which the primers bind to the introns flanking exon 3 of EXO1. If the puromycin gene was properly inserted, the PCR should yield a 1866 bp product. In contrast, if the puromycin gene was not inserted (leaving exon 3 intact), then the PCR product representing the parental locus should be 456 bp. Initially, on multiple representative clones, the puromycin insertion PCR product was much less prominent than the parental product indicating that not all of the loci were targeted (Fig. 3.5b). To resolve this issue, we performed two subsequent transfections on clone #46, yielding a total of three CRISPR/Cas9 reactions for this clone (identified as ‘U2OS EXO1 #46.3’). The puromycin insertion PCR product was extremely intense compared to the parental PCR product (Fig. 3.5c), suggesting that multiple transfections can improve efficiency. However, despite three transfections, the parental loci band still remained, albeit at a low level. The presence of the parental PCR product correlated with only a

partial reduction in EXO1 protein similar to that seen by siRNA knockdown of EXO1 (Fig. 3.5d).

U2OS cells have a hyper-triploid karyotype, perhaps making it problematic to obtain a complete knock-out using the CRISPR/Cas9 system. As an alternative approach, we used 1BR cells, which are normal human diploid fibroblasts. We obtained a pure knock-out clone (identified as ‘1BR EXO1 #2’) after just one transfection as indicated by PCR (Fig. 3.5e). However, by Western blot, at least some protein still remained (Fig. 3.5f).

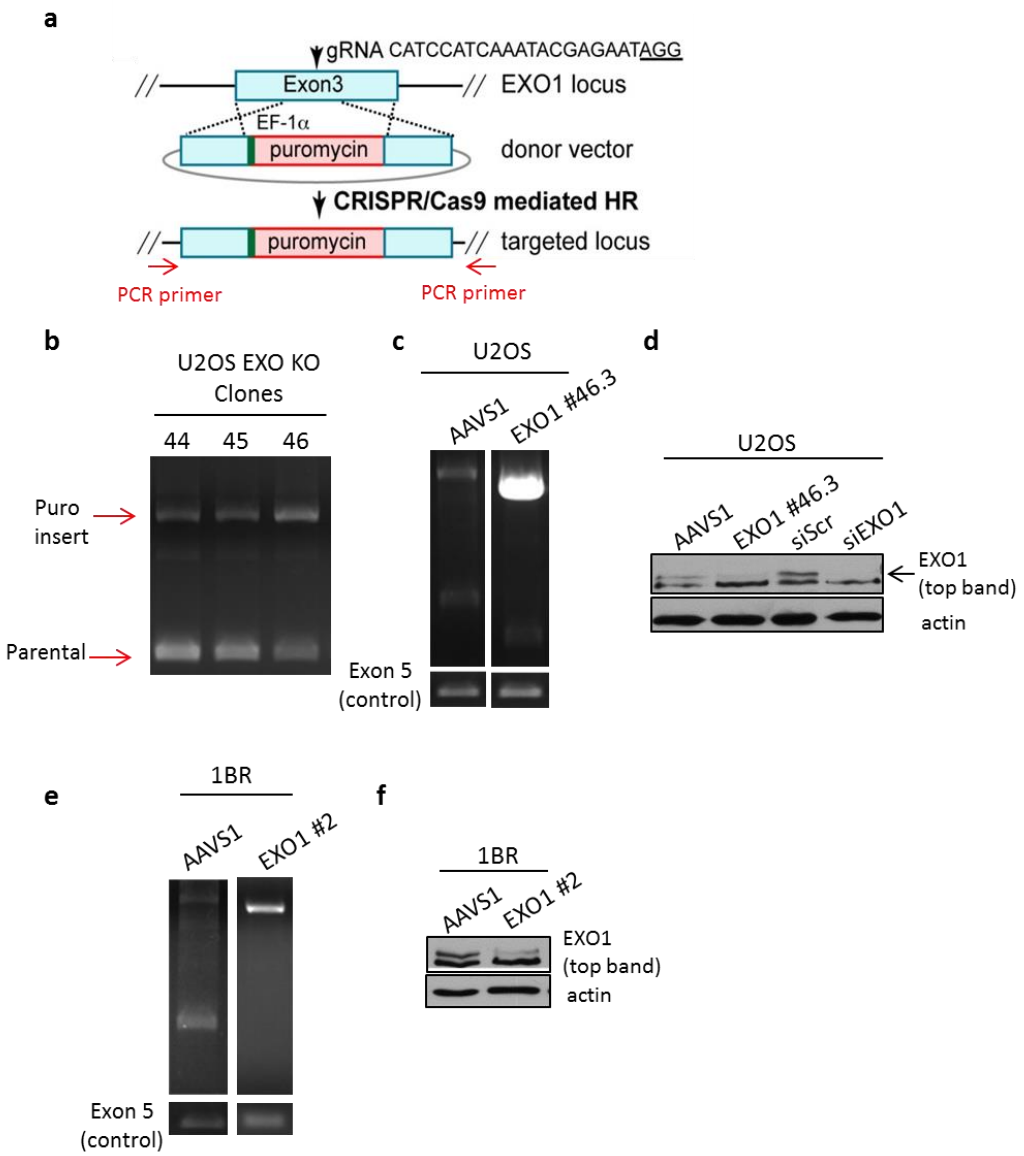

Figure 3.5. Generation of EXO1 knock-out cells for checkpoint analysis. (a) Schematic showing knock-out strategy using a guide RNA targeting exon 3 of EXO1 and a donor vector with a puromycin resistance gene. Upon transfection of the Cas9 plasmid, homologous recombination results in the insertion of the puromycin resistance gene to disrupt exon 3. (b) Representative U2OS EXO1 knockout clones were screened by PCR using primers that bind to the introns flanking exon 3 (see (a); red arrows). Both the parental loci and the targeted loci are present. (c) U2OS AAVS1 (single transfection) and EXO1 #46.3 (triple transfection) were screened by PCR. PCR of exon 5 is an internal control. (d) Western blot of endogenous EXO1 (top band) in the U2OS AAVS1 control and EXO1 #46.3 knockout lines compared to U2OS cells with scrambled siRNA and siRNA against EXO1. (Western blot was performed by Mukherjee, B.) (e) 1BR AAVS1 (single transfection) and EXO1 #2 (single transfection) were screened by PCR. PCR of exon 5 is an internal control. (f) Western blot of endogenous EXO1 (top band) in the 1BR AAVS1 control and EXO1 #2 knockout lines.

EXO1 knock-outs have an altered G2/M checkpoint

We validated the U2OS EXO1 #46.3 cell line by RPA immunofluorescence, and indeed, this partial knock-out exhibits a resection defect compared to control cells as expected (Fig. 3.6a). Interestingly, both U2OS EXO1 #46.3 (Fig. 3.6b,c) and 1BR EXO1 #2 (Fig. 3.6d) escape the G2/M checkpoint sooner than controls as indicated by an increase in phospho-histone H3+ cells at 16-24 hours after IR. However, the differences were small, most likely due to not having a complete knock-out.

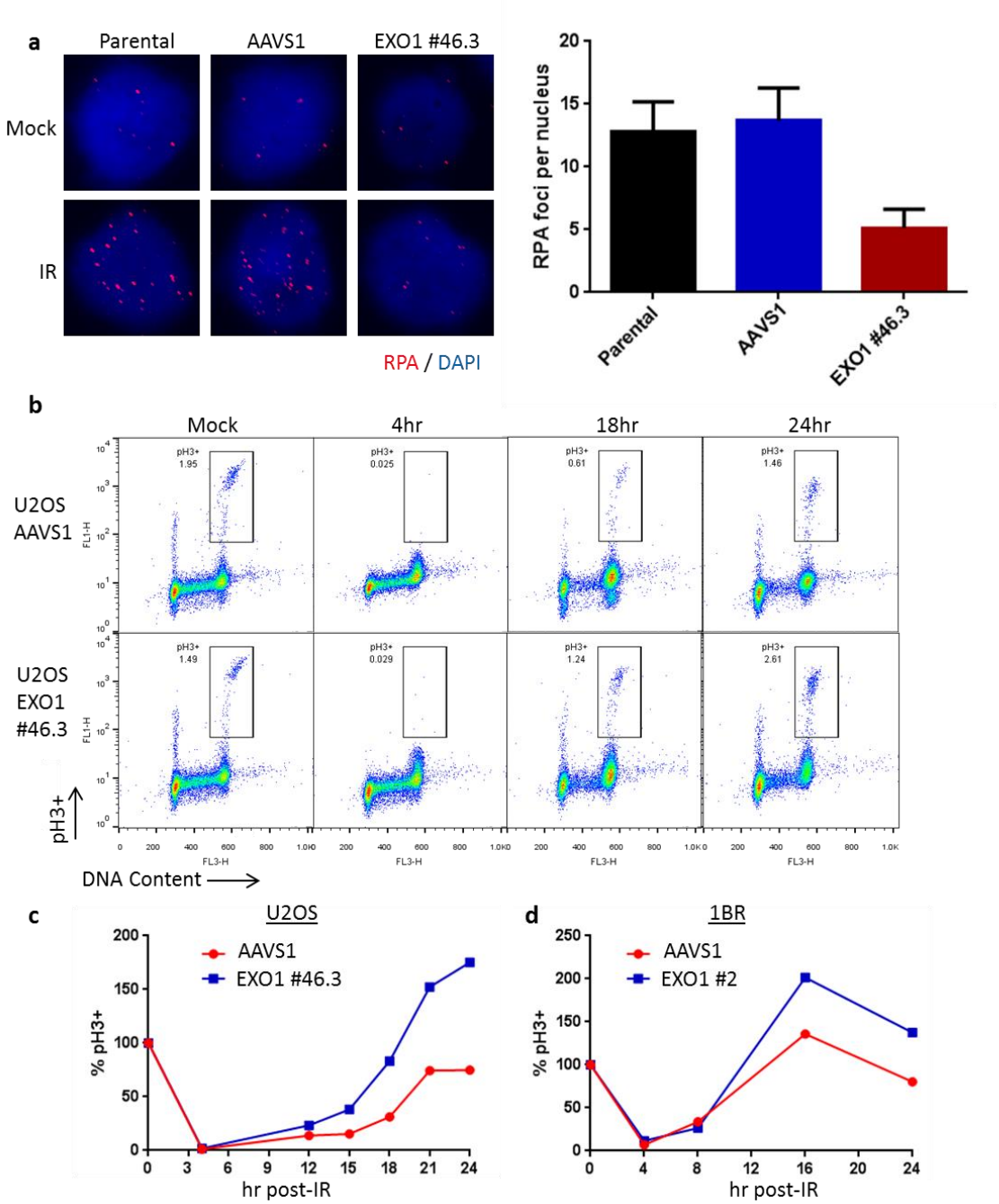

Figure 3.6. EXO1 knock-outs have an altered G2/M checkpoint. (a) U2OS parental, AAVS1, and EXO1 #46.3 knockout cells were irradiated and immunofluorescence stained for RPA to test for resection defects. (b) U2OS AAVS1 and EXO1 #46.3 knockout cells were irradiated, harvested at the indicated time points, stained for phospho-histone H3, and quantified by flow cytometry. (c) Quantification of the U2OS phospho-histone H3+ cells relative to mock from (b). (d) Quantification of flow cytometric analysis of 1BR AAVS1 and EXO1 #2 phospho-histone H3+ cells after IR relative to mock.

EXO1 knock-out may not be complete

Since the knock-outs may contain contaminant cells, we grew up clones of early passage U2OS EXO1 #46.3 and 1BR EXO #2 lines. However, in the case of the U2OS line, after about one month in culture, the PCR screen indicated that the puromycin insertion band was decreasing, while the parental band was increasing (Fig. 3.7a). This same strategy of performing three transfections, followed by growing up clones, was performed with another U2OS clone, but it exhibited the same problem of reversion to the parental loci over time (data not shown). This indicates that the reversion was not due to an obscurity in one clone, but a broader phenomenon with this cell line. As for the 1BR EXO1 #2 knock-out, the new sub-clones remained complete knock-outs by PCR (Fig. 3.7b), but some protein was still present by Western blot (Fig. 3.7c). However, clones with very low levels of EXO1 protein may suffice for future studies.

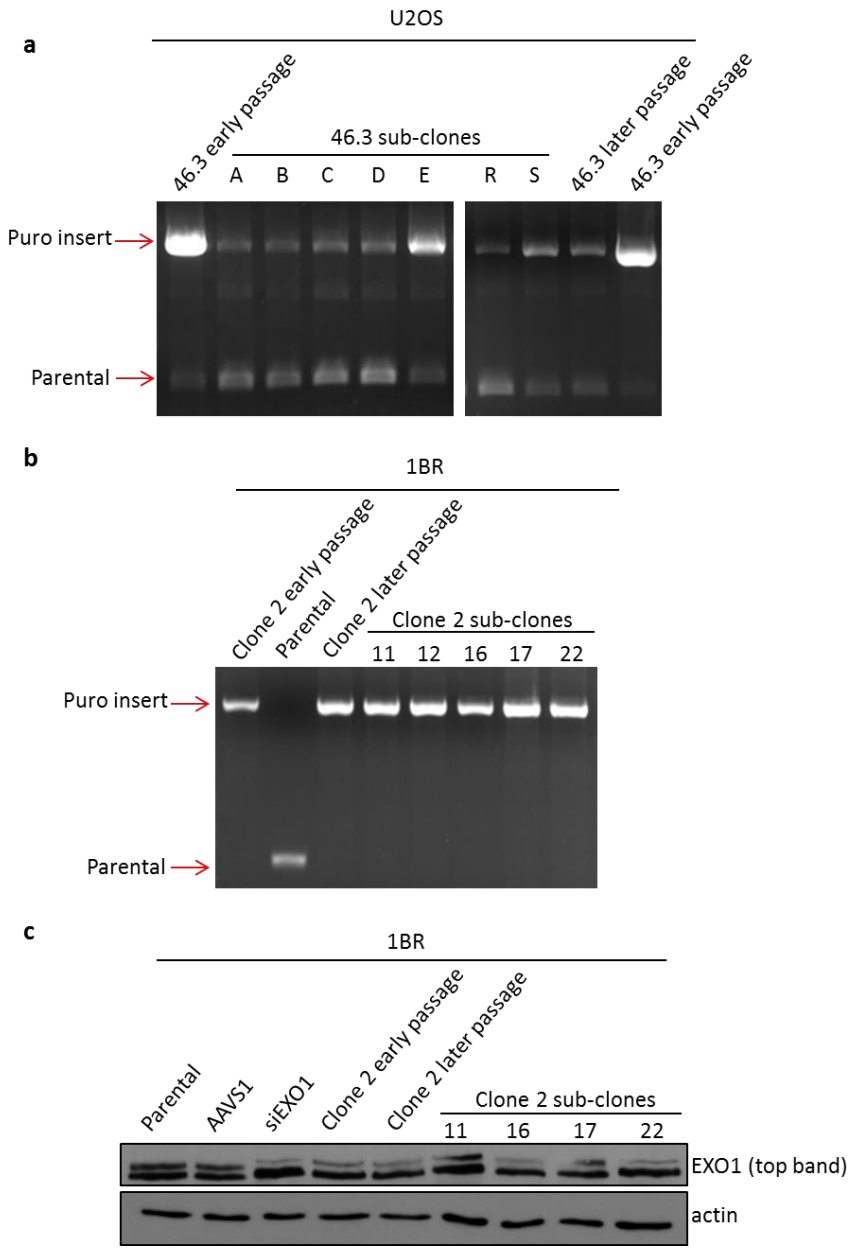

Figure 3.7. EXO1 knock-out may not be complete. (a) U2OS EXO1 #46.3 (early and late passages) and its sub-clones were analyzed by PCR for presence of the puromycin insertion and parental loci. (b) 1BR parental, 1BR EXO1 #2 (early and late passages), and 1BR EXO1 #2 sub-clones were analyzed by PCR for presence of the puromycin insertion and parental loci. (c) Western blot comparing endogenous EXO1 (top band) levels in 1BR parental, AAVS1, siEXO1, EXO1 #2, EXO1 #2 sub-clones.

Discussion

Multiple proteins bind to the C-terminus of EXO1 to regulate its function in MMR (Schmutte et al., 2001), but the protein interaction domains and post-translational modification sites on EXO1 that regulate its function during HR are largely undetermined. In this study, we reveal that the C-terminus of EXO1 is critical for its function in HR and has additional implications for the G2/M checkpoint response.

EXO1 is a member of the RAD2 nuclease family and functions in MMR, NER, and HR repair, with additional roles in DNA replication, recombination, and telomere maintenance (Tishkoff DX et al., 1998; Giannattasio et al., 2010; Bolderson et al., 2010; Tomimatsu et al., 2012; Cotta-Ramusino et al., 2005; Keelagher et al., 2011; Schaetzlein et al., 2007). The exonucleolytic N-terminal domain of EXO1 is well-conserved among the 5’ structure-specific nuclease family (Orans et al., 2011). In contrast, the C-terminus of EXO1 is divergent and not well-conserved, but contains several docking sites for mismatch repair proteins, including MSH2, MSH3, and MLH1 (Orans et al., 2011; Schmutte et al., 2001). Using these MMR studies as a guide, we generated EXO1 deletion constructs to examine the HR-relevant protein interactions and functional domains of EXO1 in vivo. We find that a construct containing the nuclease domain but lacking the C-terminal tail (d353-846) exhibits marked resection and DSB repair defects. Interestingly, this exact construct was recently crystalized in complex with a 10 base pair DNA substrate containing a 3’ single-strand extension (Orans et al., 2011). Although in vitro the nuclease domain of EXO1 can bind to DNA (Orans et al., 2011), we find that in vivo the C-terminus is required for localization to DNA and subsequent resection.

We then questioned whether HR proteins may interact with EXO1 on its C-terminus to regulate its function. Indeed we find that BLM interacts with the C-terminus of EXO1. Although we are uncertain about the functional importance of this interaction, past studies demonstrated that BLM interacts with EXO1 and increases EXO1's affinity for DNA ends (Nimonkar et al., 2008; Nimonkar et al., 2011). It is interesting to speculate that this C-terminal interaction with BLM may be important for localization of EXO1 to the break site; this would parallel a recent study from our lab demonstrating that BRCA1 interacts with EXO1 and aids in the recruitment of EXO1 to laser-induced DSBs (Tomimatsu et al., 2014). In addition to BLM interacting with the C-terminus of EXO1, we also identified four CDK phosphorylation sites that lie on the C-terminus of EXO1 and are essential for EXO1's role in resection (Tomimatsu et al., 2014). Therefore, we hypothesize that the C-terminus of EXO1 may serve as a platform for both post-translational modifications and protein interactions which regulate its function during HR.

To further examine the role of CDK phosphorylation of EXO1, we questioned how these phosphorylation events may influence the duration of the G2/M checkpoint and the order of activation of the central checkpoint kinases, ATM and ATR. Our current model system used for the resection and repair assays rely on efficient siRNA knockdown of endogenous EXO1 and a high transfection efficiency of the EXO1 mutant plasmids. This system is sufficient for short-term experiments, but monitoring of cell cycle checkpoints over an extended period of time requires a more robust and stable model system. Therefore, we are using CRISPR/Cas9 technology to generate stable EXO1 knock-out cells and will then stably express WT-, CDK-phospho-mutant-, CDK-phospho-mimic-, or nuclease dead-EXO1.

Despite a relatively simple method, we find that after three CRISPR/Cas9 transfections in U2OS cells, we still did not obtain a complete knock-out, and the targeted loci seem to revert

back to the parental loci over time. This observation was noted with two independent U2OS clones. One reason for this observation may be that cells with functional (non-targeted) EXO1 were naturally selected for and thus outgrew the targeted population. As an alternative hypothesis, in the early passage EXO1 #46.3 in which nearly every locus was targeted, the small amount of functional EXO1 protein that remained may have been sufficient to restore the originally targeted loci back to the parental state by executing HR at endogenous breaks. To test this hypothesis, one could knock-out another gene that is indispensable for HR to determine if the EXO1 knock-out (puromycin insertion) is then maintained. To circumvent this problem in U2OS cells, which have at least three copies of each gene, we used 1BR normal diploid fibroblasts. While the PCR indicated a total knockout, protein was still present by Western blot perhaps indicative of a mixed population containing unmodified cells. Alternatively, it is possible that the CRISPR/Cas9 reaction generated a new open reading frame which permits expression of the protein.

Ultimately, we will complement the EXO1 knock-out cells with WT or 4A-EXO1 to understand how CDK phosphorylation of EXO1 alters the amount of time spent in the G2/M checkpoint, in addition to the extent of activation of the ATM and ATR kinases after treatment with IR. Based on our current work demonstrating that CDK phosphorylation of EXO1 is essential for resection (Tomimatsu et al., 2014), we postulate that EXO1 knock-out cells complemented with 4A-EXO1 may have activation of ATM and an initial pause in the G2/M checkpoint; however, without CDK phosphorylation of EXO1 and subsequent resection, we expect that ATR will not be activated and cells will exit the checkpoint prematurely, leading to unrepaired or improperly repaired DNA. This hypothesis coincides with our preliminary results using the EXO1 knock-outs, which escape faster from the G2/M checkpoint compared to control

cells. However, these results will require future validation upon generation of pure EXO1 knock-outs.

In conclusion, our results demonstrate that in vivo, the exonucleolytic activity of EXO1 does not rely solely on its nuclease domain, but rather requires the C-terminal domain for localization to the break site in order for resection to ensue. We expect that proper regulation of EXO1 mediated through C-terminal protein interactions will be critical for its function in HR. We also mapped four C-terminal CDK phosphorylation sites on EXO1 that are necessary for resection (Tomimatsu et al., 2014), and based on initial results, we suspect that CDK phosphorylation of EXO1 will also be essential for proper G2/M checkpoint regulation to allow for appropriate repair and preservation of genomic stability.

Chapter IV

EXO1 breast cancer-associated SNP N279S exhibits a DSB repair defect

Introduction

Breast cancer is the most prevalent cancer among women, and approximately 10% of these cases have a hereditary component (Siegel et al., 2016; Foulkes, 2008). Some of the most commonly altered genes that give rise to inherited breast cancer are BRCA1, BRCA2, ATM, and CHK2, all of which are highly involved in the signaling and repair processes following DNA damage (Foulkes, 2008; Michailidou et al., 2015). However, these genes only account for a fraction of the inherited risk. Therefore, much effort has been dedicated to pinpoint other susceptibility loci that may promote breast cancer.

Towards this goal, a recent genome-wide association study defined 15 new breast cancer susceptibility loci through analysis of over 11 million SNPs from 120,000 women of European descent (Michailidou et al., 2015). One of the 15 SNPs resides in an EXO1 intron region, and when investigating the causal variants that underlie this SNP, they identified a SNP (N279S) in the coding region of EXO1. They predict that N279S is deleterious, meaning that it decreases organismal fitness, and thus poses a breast cancer risk (Michailidou et al., 2015; Kircher et al., 2014).

EXO1 is a 5’ to 3’ exonuclease that functions in DNA recombination and replication, in addition to multiple DNA repair pathways, including MMR and HR. With such instrumental roles in maintaining an intact genome, it’s no surprise that deletion of Exo1 in mice results in meiotic defects, decreased survival, and an increased risk of lymphoma (Wei et al., 2003). In humans, several epidemiological studies have noted EXO1 mutations leading to an increased risk of multiple cancers, including gastric, lung, breast, oral, and GBM (Bau et al., 2009; Jin et al., 2007; Michailidou et al., 2015; Wang et al., 2009; Tsai et al., 2009; Chang et al.; 2008). While

some studies have examined the contributions of EXO1 variants to MMR deficiencies, to our knowledge, there are no reports assessing EXO1 mutations in relation to its role in HR (Sun et al., 2002). EXO1's primary function in HR is to resect DNA at DSBs leaving behind a 3' ssDNA overhang that is used invade a homologous sister chromatid for error-free repair. In this study, we analyzed how the breast cancer associated EXO1 SNP, N279S, alters the DNA damage response, with a specific focus on HR. We find that EXO1 N279S exhibits striking resection and DSB repair defects, which may in the future lend interest to sensitizing cancers harboring EXO1 N279S with DNA damaging agents that require HR for repair.

Methods

Cell culture

U2OS cells were maintained in Minimal Essential Medium-alpha with 10% fetal bovine/newborn calf serum mixture and 1% penicillin/streptomycin. Cells were grown in 37˚C humidified incubators with 5% CO_2.

Mutagenesis

EXO1b was transferred from Flag2-EXO1 (Bolderson et al., 2010) into pDONR221 (Invitrogen) using BP Clonase II (Invitrogen). For mutagenesis, pDONR221/EXO1 was used as the template for the QuikChange II XL Site-Directed Mutagenesis kit (Stratagene), followed by an LR Clonase II enzyme (Invitrogen) reaction for transfer into the pLenti6.3/V5-DEST vector. See Appendix for primer sequences.

Transient transfections

Transient knockdown of EXO1 was performed using siRNA (see Appendix for sequence) that was electroporated (Lonza) into U2OS cells. Approximately 24 hours later, cells were transfected using Lipfectamine2000 (Invitrogen) with the indicated pLenti6.3/EXO1/V5 constructs and allowed to incubate for approximately 24 hours before the start of the particular assay.

DSB repair kinetics

Cells were seeded on glass 4-chamber slides (Falcon). U2OS cells were treated with 100nM CPT for 4 hours. CPT-containing media was removed and replaced with fresh media (no CPT). Cells were fixed at the indicated times using 4% paraformaldehyde. Cells were then permeabilized using 0.5% Triton X-100, blocked with 5% bovine serum albumin, and co-stained with anti-V5 (Invitrogen) and anti-53BP1 (Santa Cruz) antibodies. Cells were imaged using a Carl Zeiss Axio Imager.M2 fluorescence microscope and displayed using AxioVision Rel. SE64 4.8 software. The number of V5+ cells (or V5- cells for siRNA-sensitive WT EXO1) was scored which contained 53BP1 foci greater than the average number of 53BP1 foci in the mock sample. At least 50 cells were quantified for each sample.

Resection assay

Cells were seeded onto glass 4-chamber slides (Falcon) and irradiated with 6 Gy gamma rays using a cesium source (JL Shepherd and Associates). Three hours after IR, cells were subjected to in situ fractionation (to improve RPA foci visualization) by incubating cells on ice for 10 minutes in Extraction Buffer 1 (10mM PIPES, 100mM NaCl, 300mM sucrose, 3mM MgCl2, 1mM EGTA, and 0.5% Triton X-100), followed by a 10 minute incubation in Extraction Buffer 2 (10mM Tris (pH 7.5), 10mM NaCl, 3mM MgCl2, 1% Tween-40, and 0.5% sodium

deoxycholate). Cells were then fixed using 4% paraformaldehyde, permeabilized in 0.5% Triton X-100, blocked with 5% bovine serum albumin, and stained with anti-RPA (Calbiochem). Cells were imaged using Carl Zeiss Axio Imager.M2 fluorescence microscope and displayed using AxioVision Rel. SE64 4.8 software. Foci were quantified by counting the average number of RPA foci per nucleus and subtracting background for at least 50 cells per sample.

Live-cell imaging with laser micro-irradiation

Cells were seeded in 35 mm glass-bottom dishes (MatTek Cultureware) and transfected with GFP-EXO1-WT or -N279S plasmids, followed by overnight treatment with 10 ug/mL BrdU for sensitization to DSB break formation. Just prior to irradiation, media was replaced with CO_2-independent media (Invitrogen). Throughout the experiment, cells were maintained at 37˚C. Individual cells were micro-irradiated using a pulsed nitrogen laser (Spectra-Physics; 365 nm, 10 Hz; 80% output) and time-lapse imaged (Carl Zeiss Axiovert 200 M microscope; 63x oil immersion objective). The fluorescence at each focus and background region was measured using AxioVision Rel. SE64 4.8 software, which switches the fluorescence signal into a numeric value with arbitrary units. For each nucleus at every time interval, the background fluorescence was subtracted from the fluorescence of the accumulated GFP focus. More than 10 cells were irradiated for each sample, and the mean value was plotted for each time point.

Results

EXO1 N279S exhibits resection and DSB repair defects

We hypothesized that the EXO1 N279S SNP (Fig. 4.1a) may be associated with an increased risk of breast cancer due to an inability to resect DNA DSBs. To examine the resection capacity of this mutant, we knocked down endogenous EXO1 with siRNA and complemented

the cells with siRNA-sensitive WT EXO1 (sWT) or siRNA-resistant-WT (rWT), -N279S, or -D173A (nuclease dead) EXO1 (Fig 4.1b,c). After IR, we immunofluorescence stained for RPA and found that the N279S EXO1 SNP exhibits a resection defect similar to nuclease dead and sWT EXO1 (Fig. 4.1d). Consequently, this SNP also exhibits a severe DSB repair defect after CPT treatment, which induces replication-associated DSBs that require HR for repair (Arnaudeau et al., 2001). These results suggest that this single amino acid substitution alters the ability of EXO1 to efficiently resect and repair DNA DSBs.

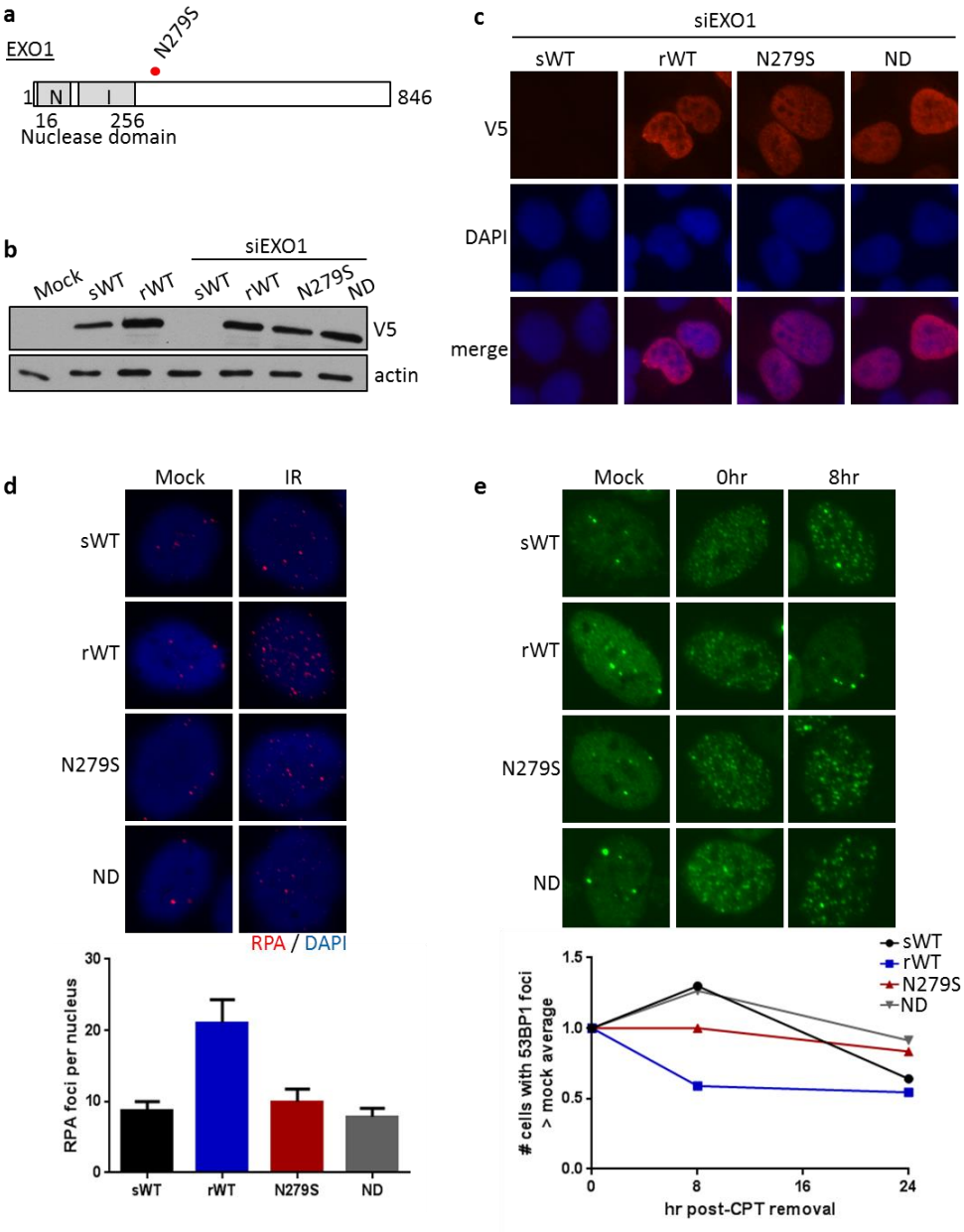

Figure 4.1. EXO1 N279S exhibits resection and DSB repair defects. (a) EXO1 schematic showing location of the N279S SNP relative to the nuclease domain. (b) U2OS cells were depleted of endogenous EXO1 by siRNA and complemented with V5-tagged siRNA-sensitive-WT EXO1 (sWT) or siRNA-resistant-WT (rWT), -N279S, or -D173A (nuclease dead (ND)) EXO1. Whole cell lysates were probed or (c) cells were immunofluorescence stained using the indicated antibodies to examine knockdown and expression levels. (d) U2OS cells with knockdown of endogenous EXO1 and expression of the indicated EXO1 plasmids were irradiated and immunofluorescence stained for RPA to visualize resection defects. (e) U2OS cells with knockdown of endogenous EXO1 and expression of the indicated EXO1 plasmids were treated with CPT for 4 hours and immunofluorescence stained for 53BP1 at the indicated times after CPT removal.

EXO1 N279S can localize to laser-induced DSBs

To determine the mechanism behind the repair defects associated with EXO1 N279S, we asked whether this mutant is capable of localizing to DSBs. To monitor localization, we micro-irradiated nuclei that expressed GFP-EXO1 WT or GFP-EXO1 N279S and tracked recruitment of EXO1 using live-cell imaging over time. We did not observe any differences in the localization kinetics (Fig. 4.2a), suggesting that N279S can localize to DSBs just as efficiently as WT EXO1. Therefore, future studies are necessary to address the mechanism by which the N279S SNP negatively affects the DSB repair capacity of EXO1.

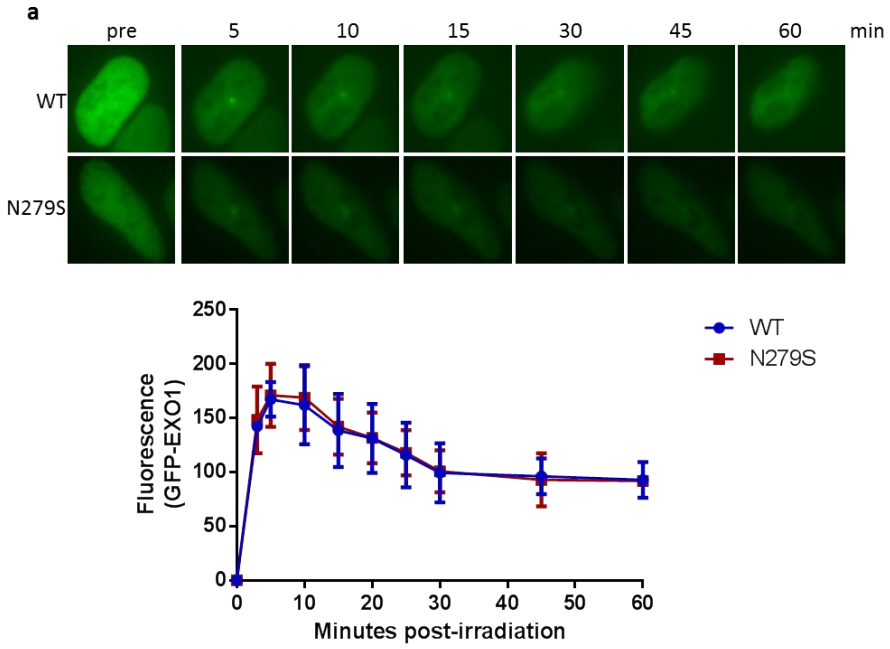

Figure 4.2. EXO1 N279S can localize to laser-induced DSBs. (a) U2OS cells were transfected with GFP-EXO1 WT or GFP-EXO1 N279S and focally irradiated to induce individual punctate DSBs with a micro-laser. GFP accumulation was monitored using live cell-imaging, and the fluorescence level was quantified after background subtraction at each time point post-irradiation.

Discussion

Nearly 20% of women diagnosed with breast cancer are estimated to succumb to the disease this year (Siegel et al., 2016). To improve the outcome for these patients, we must develop a mechanistic understanding of the molecular pathogenesis driving these tumors. A recent genome-wide association study identified 15 new breast cancer susceptibility loci, including one that correlated with an amino acid change (N279S) in the coding region of EXO1. However, this report did not characterize this EXO1 SNP to address how it may affect breast cancer progression. Since EXO1 plays a pivotal role in maintaining genomic stability through its role in HR repair, in our study, we have examined this EXO1 SNP for its capacity to respond to DNA DSBs.

We find that N279S exhibits a resection defect that culminates in attenuated DSB repair. In HR-deficient tumor cells, which is probable in cells harboring EXO1 N279S, DSBs are most likely repaired by NHEJ, thus resulting in numerous genomic alterations that could initiate carcinogenesis. In the future, in-vivo reporter assays comparing repair pathway choice could directly examine the extent to which cells expressing EXO1 N279S utilize HR versus NHEJ.

The mechanism behind the resection defect observed with EXO1 N279S remains unclear, but does not appear to be from an inability to localize to the break site. A different mechanism must exist, such the mutant altering the stability of the protein which may shorten the half-life. This could be confirmed by treating cells with cycloheximide and testing expression of N279S versus WT over time. An alternative mechanism explaining the repair defect may be due to the location of this SNP; N279 lies just outside the nuclease domain (Fig. 4.1a). Therefore, this SNP

may be directly altering the nuclease activity. In vitro nuclease assays containing purified protein with DNA substrates may provide further insight into this hypothesis.

Knowing whether a tumor has this EXO1 mutation may be useful for designing personalized treatment strategies. These patients may benefit from a synthetic lethal therapeutic approach through use of PARP inhibitors, which are currently being investigated in BRCA1/2 deficient cancers (Dedes et al., 2011; Kaufman et al., 2015). PARP inhibitors trap PARP onto single strand breaks, which during replication are converted to DSBs that require HR for proper repair (Murai et al., 2012). In cells expressing EXO1 N279S, which cannot resect DNA, PARP inhibitor-induced breaks should be left unrepaired and ultimately trigger cancer cell death.

To the best of our knowledge, this is the first time that an EXO1 SNP that is associated with cancer susceptibility has been analyzed for HR defects. It is worth noting that EXO1 N279S may exhibit defects in other pathways, such as MMR, which remain to be tested. Based on our analysis though, we find that EXO1 N279S exhibits resection and repair defects that likely lead to an increased breast cancer risk due to heightened genomic instability.

Chapter V

Conclusions and Future Directions

Our study has uncovered novel insights into DNA repair processes that have potential to influence the therapeutic strategies used to treat cancer patients. Numerous chemotherapies, in addition to radiation, promote cancer cell death through induction of DNA damage. While this can be effective in some situations, in the case of GBM, the tumors inevitably recur due to therapy resistance, suggesting that a cell population has an enhanced ability to overcome genotoxic stress and repopulate the tumor. Therefore, we must gain a better understanding of how cancer cells obtain heightened DNA repair capabilities. Previous work from our lab has unequivocally demonstrated that DNA damage itself can induce oncogenic alterations, such as Met amplification, which we find promotes a cancer stem cell phenotype, tumorigenesis, and alteration of the DNA damage response (Camacho et al., 2015).

Our finding that Met expression correlates with high Sox2 levels, neurosphere formation, and tumorigenesis validates other studies which also find that Met induces a cancer stem cell state (Li et al., 2011; Joo et al., 2012; De Bacco et al., 2012). These other studies used GBM neurosphere models with endogenous MET expression, while our model took advantage of a different approach. We irradiated the brains of mice with deletions of Ink4a, Ink4b, and Arf, which naturally induced GBMs with Met amplification (Camacho et al., 2015). We then generated ex-vivo cultures from the tumors, but loss of Met in the ex-vivo cultures necessitated ectopic re-expression. Although unfortunate, this was not too surprising since Met was in the form of double minutes which are often lost in vitro without selection from a tumor microenvironment, as observed with EGFR and EGFRvIII (Camacho et al., 2015; Bigner et al., 1990). Ectopic re-expression of Met is a clear limitation of our study due to an increased risk of

artifacts, but importantly, our model still illustrated a Met-driven cancer stem cell phenotype, thus strengthening this phenomenon.

In addition to promoting a cancer stem cell phenotype, our data indicate that Met expression correlates with high levels of DDR proteins, including the checkpoint kinases Chk1 and Chk2, suggesting that Met signaling may alter cell cycle arrest. Indeed, we found that Met-expressing cells have a prolonged G2/M checkpoint after IR. We hypothesize that this hiatus in G2 phase may allow for faithful repair of the damage through use of the error-free (and time consuming) HR pathway. Evidence for this hypothesis stems from Lim et al. who demonstrated that upon DNA damage, glioma-initiating cells bypass the G1 checkpoint to permit entry into S phase to allow HR to accurately repair the damage (Lim et al., 2012). They report that HR repair takes 12-24 hours, which although not tested, suggests that these glioma-initiating cells must have a prolonged checkpoint to allow for repair, which would be consistent with our results. Evaluation of repair pathway choice in our model would provide clarity regarding the necessity of a prolonged checkpoint.

Overall, our findings that Met expression promotes a cancer stem cell phenotype and an altered DDR have strong clinical relevance. Recurrent GBMs arise from cells that escape the effects of therapy. We hypothesize that these radioresistant cells are likely to have Met expression based on our previous findings and others showing that IR induces Met amplification and protein expression (Camacho et al., 2015; Joo et al., 2012). Our work sets the stage for a potential mechanism by which Met expression rewires cells to self-renew and equips them with a DDR that is primed to combat damage through use of excess DDR proteins and a prolonged G2/M arrest. Therefore, patients with high Met levels, especially in recurrent tumors, may

benefit from Met inhibitor therapy, such as Tivantinib which is in Phase III clinical trials for non-small cell lung cancer (Finisguerra et al., 2016).

In order to advance our study, these results should be replicated in other models that are more realistic of a human scenario, such as in human GBM neurospheres with MET expression or in human GBM cell lines with either ectopic MET expression or knock-in of MET. Our model should also be evaluated for orthotopic tumor growth rather than sub-cutaneous tumor formation to better validate our cancer stem cell hypothesis. Then, these models and our current model could be analyzed for enhanced DSB repair kinetics, repair pathway usage, radioresistance, and radiosensitization with MET inhibitors. In all, our results provide a foundation for future studies regarding MET as a driver of an augmented DDR that may propel radioresistance of cancer stem cells, thus making MET a rational target for cancer therapies.

In addition to targeting oncogenes, patients with radioresistant tumors may benefit from directly targeting DNA repair proteins. To develop therapeutic strategies that impinge on DNA repair processes, we must acquire a detailed insight on how individual protein domains and interactions affect the function of key DNA repair proteins. We have accomplished this through examination of the domains of EXO1, a primary exonuclease in the HR repair pathway. We find that the C-terminus of EXO1 is critical for damage site localization, resection, and DSB repair. Furthermore, the C-terminus serves as a platform for an interaction with BLM helicase and CDK phosphorylation sites. The C-terminus acting as a platform for protein interactions also occurs during MMR (Schmutte et al., 2001), suggesting that the C-terminus regulates the nuclease activity through multiple protein interactions that are specific to the damage type. In support of this model, it was recently postulated that during MMR, the C-terminus acts as an auto-inhibitory domain that directly restricts nuclease activity, but can be released through a C-terminal

interaction with MutSα to permit nucleolytic activity at the region containing mismatched DNA (Orans et al., 2011). Therefore, HR-relevant protein interactions with the C-terminus may serve a similar purpose to modulate the exonucleolytic activity of EXO1.

The C-terminal EXO1-BLM interaction we observe does have some limitations. This interaction is dependent upon treatment with the proteasome inhibitor, MG132, in addition to the Topoisomerase I inhibitor, camptothecin. This suggests that the interaction may be transient, but can be prolonged by inhibition of degradation machinery. However, this result provides new insights regarding the regulation of EXO1, which could be bolstered by future work addressing this interaction and others, such as with CtIP and BRCA1, in the presence or absence of DNA damage and/or MG132. Knockdown of BLM may also help discern how BLM affects the localization and nucleolytic efficiency of EXO1. Additionally, we did not find conclusive interactions using the other deletion fragments of EXO1 (Fig 3.1a). This may suggest that the interactions are transient or span multiple domains on EXO1. Future studies may require altering the deleted regions of the constructs or optimization of the immunoprecipitation conditions to detect such interactions.

In addition to BLM interacting with the C-terminus of EXO1, we also mapped four CDK phosphorylation sites on EXO1's C-terminus. Work from our lab has demonstrated that CDK1 and CDK2 phosphorylation of EXO1 in S and G2 phases promotes DNA-end resection and repair pathway choice by promoting HR and suppressing NHEJ (Tomimatsu et al., 2014), thus strongly coupling resection to the cell cycle. Just as the process of resection must have multiple levels of regulation to prevent unwarranted nuclease activity, it is logical that cell cycle arrest must also be stringently controlled to ensure that cells do not slip through the checkpoint without proper DNA repair. Therefore, we asked to what extent CDK phosphorylation of EXO1

regulates the order of activation of the ATM and ATR kinases and the duration of the G2/M checkpoint. Although we are currently working towards generating the appropriate cell lines to answer this question, we have preliminary results suggesting that EXO1-null cells, which display a resection defect, escape the G2/M checkpoint faster than control cells. We must be cautious with this finding since the knock-out genotype was not maintained over time, but the result does mimic what we would expect with CDK-phospho-mutant EXO1 (4A-EXO1), which is also deficient in resection (Tomimatsu et al., 2014). Such results would parallel the recent report demonstrating that upon DNA damage, CDK phosphorylation of CHK1 promotes CHK1 activation and checkpoint proficiency, and mutation of the CDK phosphorylation sites causes cells to bypass the G2/M arrest and enter into mitosis (Xu et al., 2012). This report and our expected results suggest that CDKs act on multiple DDR substrates to restrict damaged cells from entering mitosis and thus maintain the G2/M checkpoint to allow time for repair. To examine this further, we must obtain complete EXO1 knock-outs so that we can express CDK-phospho-mutant-EXO1 (or WT-, CDK-phospho-mimic-, or nuclease dead-EXO1 controls). We are currently testing the 1BR EXO1 #2.16 sub-clone, which only has minimal EXO1 protein (Fig. 3.7c). Additionally, we are testing cells from a recent publication which developed EXO1 knock-out cells using a different CRISPR/Cas9 approach that co-targets the HPRT gene to enrich for EXO1 knock-outs (Liao et al., 2015). Once we have validated the EXO1 knock-out cells and obtain stable expression of the appropriate EXO1 constructs, we can analyze G2/M arrest by phospho-histone H3 levels and compare checkpoint signaling through activation of ATM, ATR, and their downstream substrates over time.

With EXO1 having essential roles in DSB repair and checkpoint maintenance, mutations in EXO1 may have a negative impact on genome stability and possibly predispose people to

carcinogenesis. An EXO1 SNP (N279S) was recently identified and associated with an increased breast cancer risk (Michailidou et al., 2015). Upon characterization, we found that EXO1 N279S can localize to laser-induced DSBs, but cannot resect DNA, leading to a repair defect. Our finding mirrors those reported in a MMR study examining two hereditary colorectal cancer mutations in EXO1, E109K and L410R; these mutations display attenuated nuclease activity but can bind DNA in vitro (Sun et al., 2002). Although we find a repair defect with N279S, one caveat of our investigation is that the defect was restricted to a four hour treatment with 100nM CPT; when we tested 10nM CPT for two hours (data not shown), no differences were observed, suggesting a threshold effect. The data using a low CPT dose were preliminary and must be repeated; however, if true, it may suggest that these low dose CPT-induced breaks may be repaired independently of EXO1 by utilizing the DNA2/BLM resection pathway. In contrast, when cells are faced with higher CPT doses, resulting in extreme DNA damage, other resection mechanisms may become exhausted and depend on EXO1; therefore, cells expressing N279S would display a repair defect. In the future, one should examine the differences in repair pathway usage in cells expressing N279S when faced with various levels of damaging agents. Additionally, we recommend testing the sensitization of N279S cells when treated with DNA damaging agents that require HR for repair, since this synthetic lethal approach may improve the outcome of patients presenting this mutation.

To summarize the EXO1 studies, we have demonstrated how the C-terminus of EXO1 is essential for in vivo DNA DSB localization, resection, and repair. The C-terminus also facilitates an interaction with BLM and contains four CDK phosphorylation sites. Additionally, we propose that CDK phosphorylation of EXO1 may modulate the duration of the G2/M checkpoint based on our preliminary results with EXO1 knock-out lines. Lastly, we find that the breast cancer-

associated EXO1 SNP, N279S, causes resection and DSB repair defects. Our conclusions have therapeutic relevance, as tumors that are radioresistant due to enhanced HR, such as the glioma-initiating cells described by Lim et al., may benefit from EXO1 inhibition (Lim et al., 2012). However, no EXO1 inhibitors currently exist. Based on our data, inhibitors designed to target either the N-terminus or the C-terminus should be effective at preventing the exonucleolytic activity of EXO1, thus blocking HR repair. Alternatively, since CDKs are essential for EXO1's function and CDK1 and CDK2 inhibitors are currently in clinical trials, we hypothesize an effective radiosensitization strategy may include treating HR-proficient tumors with CDK1 and CDK2 inhibitors. Indeed, unpublished work from our lab supports this hypothesis. In contrast, patients with HR-defective tumors, such as those who bear the EXO1 N279S SNP, may benefit from treatment with CPT or PARP inhibitors, which require HR for repair.

Overall, this thesis illuminates new DNA repair insights by examining how damage-induced oncogenic alterations can affect the DDR and how a specific DDR protein, EXO1, is regulated and functions in response to genomic instability. These insights provide a stepping-stone for new studies that address the therapeutic potential of MET inhibitors and strategies to target EXO1 or the proteins with which it interacts to ultimately give cancer patients a fighting chance against such a complex disease.

APPENDIX A

Primer, siRNA, and gRNA target sequences

Table 1: EXO1 mutagenesis and deletion construct primer sequences

rWT EXO1	TCACTGCGTGGGATTGGTCTTGCAAAGGCATGCAAAGTCC
EXO1 d1-401	attB2 F: GGGGACAAGTTTGTACAAAAAAGCAGGCTTCACC***ATG***ACTAAAGGGTTAAATCTCCCA attB2 R: GGGGACCACTTTGTACAAGAAAGCTGGGTTCTGGAATATTGCTCTTTG
EXO1 d353-445	attB1 F: GGGGACAAGTTTGTACAAAAAAGCAGGCTTCACC***ATG***GGGATACAGGGATTGCTA Internal R: CAATGATTTATTGCCTTCAGAGCTTCTTGAATGGGCAGGCATAGCAGT Internal F: ACTGCTATGCCTGCCCATTCAAGAAGCTCTGAAGGCAATAAATCATTG attB2 R: GGGGACCACTTTGTACAAGAAAGCTGGGTTCTGGAATATTGCTCTTTG
EXO1 d446-638	attB1 F: GGGGACAAGTTTGTACAAAAAAGCAGGCTTCACC***ATG***GGGATACAGGGATTGCTA Internal R: ATTCTCAGGCAAAGAGGTGGGGGAATTTTTCTTGGTCTTCTTCGTAAA Internal F: TTTACGAAGAAGACCAAGAAAAATTCCCCCACCTCTTTGCCTGAGAAT attB2 R: GGGGACCACTTTGTACAAGAAAGCTGGGTTCTGGAATATTGCTCTTTG
EXO1 d639-846	attB1 F: GGGGACAAGTTTGTACAAAAAAGCAGGCTTCACC***ATG***GGGATACAGGGATTGCTA attB2 R: GGGGACCACTTTGTACAAGAAAGCTGGGTTATCGCTCTTTCTTCGGAA
EXO1 d353-846	attB1 F: GGGGACAAGTTTGTACAAAAAAGCAGGCTTCACC***ATG***GGGATACAGGGATTGCTA attB2 R: GGGGACCACTTTGTACAAGAAAGCTGGGTTTCTTGAATGGGCAGGCAT
EXO1 S376A	TTGGCATAGGAATTACGCTCCCAGACCAGAGTCGGGTACTGTTT
EXO1 T475A	CAAAAAGAGTGTAAGCGCCCCACCTAGGACGAGAAATAAATTTG
EXO1 S598A	CAAATTTACAAGGACCATTGCACCACCCACTTTGGGAACACTAA
EXO1 T621A	TGGAGATTTTTCAAGAGCGCCGAGCCCCTCTCCAAGCACAGCAT
EXO1 S623A	TGGAGATTTTTCAAGAACGCCGGCCCCCTCTCCAAGCACAGCAT
EXO1 S625A	AGAACGCCGAGCCCCGCTCCAAGCACAGCATTGCAG
EXO1 S639A	GTTCCGAAGAAAGAGCGATGCCCCCACCTCTTTGCCTGAGAATA
EXO1 T732A	TTTCTCAAAAAAAGACGCACCTCTAAGGAACAAGGTTCCTGGGC
EXO1 S815A	TTGTAAGAAACCCCTGGCCCCAGTCAGAGATAACATCCAACTAA
EXO1 T824D	CAGAGATAACATCCAACTAGCTCCAGAAGCGGAAGAGGATATAT
EXO1 D173A (ND)	ATAATTACAGAGGACTCGGCTCTCCTAGCTTTTGGCTG
EXO1 N279S	ATCAACGGGTTTATTCGGGCCAACAATACCTTCCTCTATCAGCTAGTT

Table 2: EXO1 siRNA sequences

siEXO#1	UGCCUUUGCUAAUCCAAUCCCACGC
siEXO#2	UAGUGUUUCAGGAUCAACAUCAUCU
siEXO#3	UUUGUUAGUAGGUCCAUUUACCAGG

Table 3: gRNA target sequences

EXO1	CCTATTCTCGTATTTGATGGATG
AAVS1	GGGCCGGTTAATGTGGCTC

Table 4: Knock-out PCR screening strategy primer sequences

EXO1 knock-out for puromycin insert versus parental locus	F: CAGACATCACATGGCTCGTAAGTATC R: CTCCCGAGTACCTAGGACAAC
EXO1 exon 5	F: GCT GCC CGG TCT CAG GGG GTA R: CAGCCAAAAGCTAGGAGATCCG
AAVS1 knock-out for puromycin insert versus parental locus	F: CTTTCCGGAGCACTTCCTTC R: CCAATCCTGTCCCTAGTGGC

BIBLIOGRAGHY

Arnaudeau C, Lundin C, Helleday T (2001) DNA double-strand breaks associated with replication forks are predominantly repaired by homologous recombination involving an exchange mechanism in mammalian cells. *Journal of Molecular Biology* 307:1235-1245.

Bakkenist C, Kastan M (2003) DNA damage activates ATM through intermolecular autophosphorylation and dimer dissociation. *Nature* 421:499-506.

Barber LJ, Youds JL, Ward JD, Mcllwraith MJ, O'Neil NJ, Petalcorin MI *et al* (2008) RTEL1 maintains genomic stability by suppressing homologous recombination. *Cell* 135:261-271.

Bau D, Wang H, Liu C, Chang C, Chiang S, Wang R *et al* (2009) Single-nucleotide polymorphism of the Exo1 gene: Association with gastric cancer susceptibility and interaction with smoking in Taiwan. *Chinese Journal of Physiology* 52:411-418.

Bartek J, Lukas C, Lukas J (2004) Checking on DNA damage in S phase. *Nature Reviews Molecular Cell Biology* 5:792-804.

Bartek J, Lukas J (2001) Mammalian G1- and S-phase checkpoints in response to DNA damage. *Current Opinion in Cell Biology* 13:738-747.

Beroukhim R, Getz G, Nghiemphu L, Barretina J, Hsueh T, Linhart D *et al* (2007) Assessing the significance of chromosomal aberrations in cancer: Methodology and application to glioma. *Proceedings of the National Academy of Sciences* 104:20007-20012.

Bhat KP, Balasubramaniyan V, Vaillant B, Ezhilarasan R, Hummelink K, Hollingsworth F *et al* (2013) Mesenchymal differentiation mediated by NF-κB promotes radiation resistance in glioblastoma. *Cancer Cell* 24:331-346.

Bigner SH, Humphrey PA, Wong AJ, Vogelstein B, Mark J, Friedman HS *et al* (1990) Characterization of the epidermal growth factor receptor in human glioma cell lines and xenografts. *Cancer Research* 50:8017-8022.

Bolderson E, Tomimatsu N, Richard DJ, Boucher D, Kumar R, Pandita TK *et al* (2010) Phosphorylation of Exo1 modulates homologous recombination repair of DNA double-strand breaks. *Nucleic Acids Research* 38:1821-1831.

Calvin LW, Dalrymple GV, McGuire EL, Maners AW, Broadwater JR (1990) CNS tumor induction by radiotherapy: A report of four new cases and estimate of dose required. *International Journal of Radiation Oncology, Biology, Physics* 28:399-406.

Camacho CV, Todorova PK, Hardebeck MC, Tomimatsu N, Gil del Alcazar CR, Ilcheva M *et al* (2015) DNA double-strand breaks cooperate with loss of Ink4 and Arf tumor suppressors to generate glioblastomas with frequent Met amplification. *Oncogene* 34:1064-1072.

Chang JS, Yeh R, Wiencke JK, Wiemels JL, Smirnov I, Pico AR et al (2008) Pathway analysis of single-nucleotide polymorphisms potentially associated with glioblastoma multiforme susceptibility using random forests. *Cancer Epidemiology, Biomarkers & Prevention* 17:1368-1373.

Chen J, Li Y, Yu TS, McKay RM, Burns DK, Kernie SG *et al* (2012) A restricted cell population propagates glioblastoma growth after chemotherapy. *Nature* 488:522-527.

Chen L, Nievera CJ, Lee AY, Wu X (2008) Cell cycle-dependent complex formation of BRCA1.CtIP.MRN is important for DNA double-strand break repair. *The Journal of Biological Chemistry* 283:7713-7720.

Chen X, Kim IK, Honaker Y, Paudyal SC, Koh WK, Sparks M et al (2015) 14-3-3 proteins restrain the Exo1 nuclease to prevent overresection. *The Journal of Biological Chemistry* 290:12300-12312.

Chen X, Niu H, Chung WH, Zhu Z, Papusha A, Shim EY *et al* (2011) Cell cycle regulation of DNA double-strand break end resection by Cdk1-dependent Dna2 phosphorylation. *Nature Structural & Molecular Biology* 18:1015-1019.

Chen X, Paudyal SC, Chin RI, You Z (2013) PCNA promotes processive DNA end resection by Exo1. *Nucleic Acids Research* 41:9325-9338.

Ciccia A, Elledge SJ (2010) The DNA damage response: Making it safe to play with knives. *Molecular Cell* 40:179-204.

Costanzo V, Shechter D, Lupardus PJ, Cimprich KA, Gottesman M, Gautier J (2003) An ATR- and Cdc7-dependent DNA damage checkpoint that inhibits initiation of DNA replication. *Molecular Cell* 11:203-213.

Cotta-Ramusino C, Fachinetti D, Lucca C, Doksani Y, Lopes M, Sogo J *et al* (2005) Exo1 processes stalled replication forks and counteracts fork reversal in checkpoint-defective cells. *Molecular Cell* 17:153-159.

Davies OR, Pellegrini L (2007) Interaction with the BRCA2 C terminus protects RAD51-DNA filaments from disassembly by BRC repeats. *Nature Structural & Molecular Biology* 14:475-483.

Davis AJ, Chen DJ (2013) DNA double strand break repair via non-homologous end-joining. *Translational Cancer Research* 2:130-143.

De Bacco F, Casanova E, Medico E, Pellegatta S, Orzan F, Albano R *et al* (2012) The MET oncogene is a functional marker of a glioblastoma stem cell subtype. *Cancer Research* 72:4537-4550.

Dedes KJ, Wilkerson PM, Wetterskog D, Weigelt B, Ashworth A, Reis-Filho JS (2011) Synthetic lethality of PARP inhibition in cancers lacking BRCA1 and BRCA2 mutations. *Cell Cycle* 10:1192-1199.

Dunn GP, Rinne ML, Wykosky J, Genovese G, Quayle SN, Dunn IF *et al* (2012) Emerging insights into the molecular and cellular basis of glioblastoma. *Genes & Development* 26:765-784.

Eid W, Steger M, El-Shemerly M, Ferretti LP, Peňa-Diaz J, König C *et al* (2010) DNA end resection by CtIP and exonuclease 1 prevents genomic instability. *EMBO Reports* 11:962-968.

Esashi F, Christ N, Gannon J, Liu Y, Hunt T, Jasin M *et al* (2005) CDK-dependent phosphorylation of BRCA2 as a regulatory mechanism for recombinational repair. *Nature* 434:598-604.

Falck J, Forment JV, Coates J, Mistrik M, Lukas J, Bartek J *et al* (2012) CDK targeting of NBS1 promotes DNA-end resection, replication restart and homologous recombination. *EMBO Reports* 13:561-568.

Falck J, Mailand N, Syljuåsen RG, Bartek J, Lukas J (2001) The ATM-Chk2-Cdc25A checkpoint pathway guards against radioresistant DNA synthesis. *Nature* 410:842-847.

Finisguerra V, Prenen H, Mazzone M (2016) Preclinical and clinical evaluation of MET functions in cancer cells and in the tumor stroma. *Oncogene* 1-11.

Foulkes, WD (2008) Inherited susceptibility to common cancers. *The New England Journal of Medicine* 359:2143-2153.

Gastaldi S, Comoglio PM, Trusolino L (2010) The Met oncogene and basal-like breast cancer: another culprit to watch out for? *Breast Cancer Research* 12:208.

Giannattasio M, Follonier C, Tourriere H, Puddu F, Lazzaro F, Pasero P *et al* (2010) Exo1 competes with repair synthesis, converts NER intermediates to long ssDNA gaps, and promotes checkpoint activation. *Molecular Cell* 40:50-62.

Goodarzi AA, Yu Y, Riballo E, Doughlas P, Walker SA, Ye R *et al* (2006) DNA-PK autophosphorylation facilitates Artemis endonuclease activity. *The EMBO Journal* 25:3880-3889.

Gwon GH, Jo A, Baek K, Jin KS, Fu Y, Lee JB *et al* (2014) Crystal structures of the structure-selective nuclease Mus81-Eme1 bound to flap DNA substrates. *The EMBO Journal* 33:1061-1072.

Haber JE (1999) DNA recombination: the replication connection. *Trends in Biochemical Sciences* 24:271-275.

Hammel M, Yu Y, Mahaney BL, Cai B, Ye R, Phipps BM *et al* (2010) Ku and DNA-dependent Protein Kinase dynamic conformations and assembly regulate DNA binding and the initial non-homologous end joining complex. *The Journal of Biological Chemistry* 285:1414-1423.

Hanahan D, Weinberg RA (2011) Hallmarks of cancer: the next generation. *Cell* 144:646-674.

Helleday T, Eshtad S, Nik-Zainal S (2014) Mechanisms underlying mutational signatures in human cancers. *Nature Reviews Genetics* 15:585-598.

Huertas P, Jackson SP (2009) Human CtIP mediates cell cycle control of DNA end resection and double strand break repair. *The Journal of Biological Chemistry* 284:9558-9565.

Jazayeri A, Falck J, Lukas C, Bartek J, Smith GC, Lukas J *et al* (2005) ATM- and cell cycle-dependent regulation of ATR in response to DNA double-strand breaks. *Nature Cell Biology* 8:37-45.

Jin G, Wang H, Hu Z, Liu H, Sun W, Ma H *et al* Potentially functional polymorphisms of EXO1 and risk of lung cancer in a Chinese population: A case-control analysis. *Lung Cancer* 60:340-346.

Joo KM, Jin J, Kim E, Kim KH, Kim Y, Kang BG *et al* (2012) MET signaling regulates glioblastoma stem cells. *Cancer Research* 72:3828-38.

Kastan MB, Lim D (2000) The many substrates and functions of ATM. *Nature Reviews Molecular Cell Biology* 1:179-186

Kaufman B, Shapira-Frommer R, Schmutzler RK, Audeh MW, Friedlander M, Balmaña *et al* (2015) Olaparib monotherapy in patients with advanced cancer and a germline BRCA1/2 mutation. *Journal of Clinical Oncology* 33:244-250.

Keelagher RE, Cotton VE, Goldman AS, Borts RH (2011) Separable roles for Exonuclease I in meiotic DNA double-strand break repair. *DNA Repair (Amst)* 10:126-137.

Kim SH, Joshi K, Ezhilarasan R, Myers TR, Siu J, Gu C *et al* (2015) EZH2 protects glioma stem cells from radiation-induced cell death in a MELK/FOXM1-dependent manner. *Stem Cell Reports* 4:226-238.

Kircher M, Witten DM, Jain P, O'Roak BJ, Cooper GM, Shendure J (2014) A general framework for estimating the relative pathogenicity of human genetic variations. *Nature Genetics* 46:310-315.

Kong DS, Song SY, Kim DH, Joo KM, Yoo JS, Koh JS et al (2009) Prognostic significance of c-Met expression in glioblastomas. *Cancer* 115:140-148.

Koschut D, Richert L, Pace G, Niemann HH, Mély Y, Orian-Rousseau V (2016) Live cell imaging shows hepatocyte growth factor-induced Met dimerization. *Biochimica et Biophysica Acta* 1863:1552-1558.

Lathia JD, Mack SC, Mulkearns-Hubert EE, Valentim CL, Rich JN (2015) Cancer stem cells in glioblastoma. *Genes & Development* 29:1203-1217.

Lee BI, Wilson DM (1999) The RAD2 domain of human exonuclease 1 exhibits 5' to 3' exonuclease and flap structure-specific endonuclease activities. *The Journal of Biological Chemistry* 274:37763-37769.

Lee JK, Paull TT (2005) ATM activation by DNA double-strand breaks through the Mre11-Rad50-Nbs1 complex. *Science* 308:551-554.

Longati P, Bardelli A, Ponzetto C, Naldini L, Comoglio PM (1994) Tyrosines 1234-1235 are critical for activation of the tyrosine kinase encoded by the MET proto-oncogene (HGF receptor). *Oncogene* 9:49-57.

Li Y, Li A, Glas M, Lal B, Ying M, Sang Y, *et al* (2011) c-Met signaling induces a reprogramming network and supports the glioblastoma stem-like phenotype. *Proceedings of the National Academy of Sciences* 108:9951-9956.

Liao S, Tammaro M, Yan H (2015) Enriching CRISPR-Cas9 targeted cells by co-targeting the HPRT gene. *Nucleic Acids Research* 43:e134.

Liberti SE, Andersen SD, Wang J, May A, Miron S, Perderiset M *et al* (2011) Bi-directional routing of DNA mismatch repair protein human exonuclease 1 to replication foci and DNA double strand break. *DNA Repair (Amst)* 10:73-86.

Lim YC, Roberts TL, Day BW, Harding A, Kozlov S, Kijas AW *et al* (2012) A role for homologous recombination and abnormal cell-cycle progression in radioresistance of glioma-initiating cells. *Molecular Cancer Therapeutics* 11:1863-1872.

Liu Q, Guntuku S, Cui X, Matsuoka S, Cortez D, Tarnai K et al (2000) Chk1 is an essential kinase that is regulated by Atr and required for the G2/M DNA damage checkpoint. *Genes & Development* 14:1448-1459.

Lock LS, Frigault MM, Saucier C, Park M (2003) Grb2-independent recruitment of Gab1 requires the C-terminal lobe and structural integrity of the Met receptor kinase domain. *The Journal of Biological Chemistry* 278:30083-30090.

Louis DN, Ohgaki H, Wiestler OD, Cavenee WK, Burger PC, Jouvet A *et al* (2007) The 2007 WHO Classification of Tumours of the Central Nervous System. *Acta Neuropathologica* 114:97-109.

Mahaney BL, Meek K, Lees-Miller SP (2009) Repair of ionizing radiation-induced DNA double strand-breaks by non-homologous end-joining. *The Biochemical Journal* 417:639-650.

Matos J, West SC (2014) Holliday junction resolution: regulation in space and time. *DNA Repair (Amst)* 19:176-181.

Matsuoka S, Rotman G, Ogawa A, Shiloh Y, Tamai K, Elledge SJ (2000) Ataxia telangiectasia-mutated phosphorylates Chk2 in vivo and in vitro. *Proceedings of the National Academy of Sciences* 97:10389-10394.

McGowan CH, Russell P (1995) Cell cycle regulation of human WEE1. *The EMBO Journal* 14:2166-2175.

Michailidou K, Beesley J, Lindstrom S, Canisius S, Dennis J, Lush MJ *et al* (2015) Genome-wide association analysis of more than 120,000 individuals identifies 15 new susceptibility loci for breast cancer. *Nature Genetics* 47:373-380.

Murai J, Huang SY, Das BB, Renaud A, Zhang Y, Doroshow JH *et al* (2012) Trapping of PARP1 and PARP2 by clinical PARP inhibitors. *Cancer Research* 72:5588-5599.

Muthuswami M, Ramesh V, Banerjee S, Thangaraj V, Periasamy J, Rao DB *et al* Breast tumors with elevated expression of 1q candidate gene confer poor clinical outcome and sensitivity to Ras/PI3K inhibition. *PLoS One* 8:e77553.

Myler LR, Gallardo IF, Zhou Y, Gong F, Yang SH, Wold MS et al (2016) Single-molecule imaging reveals the mechanism of Exo1 regulation by single-stranded DNA binding proteins. *Proceedings of the National Academy of Sciences* 113:1170-1179.

Neglia JP, Robinson LL, Stovall M, Liu Y, Packer RJ, Hammond S *et al* (2006) New primary neoplasms of the central nervous system in survivors of childhood cancer: a report from the Childhood Cancer Survivor Study. *Journal of the National Cancer Institute* 98:1528-1537.

Nguyen L, Holgado-Madruga M, Maroun C, Fixman ED, Kamikura D, Fournier T, *et al* (1997) Association of the multisubstrate docking protein Gab1 with the hepatocyte growth factor receptor requires a functional Grb2 binding site involving tyrosine 1356. *The Journal of Biological Chemistry* 15:20811-20819.

Nimonkar AV, Genschel J, Kinoshita E, Polaczek P, Campbell JL, Wyman C *et al* (2011) BLM-DNA2-RPA-MRN and EXO1-BLM-RPA-MRN constitute two DNA end resection machineries for human DNA break repair. *Genes & Development* 25:350-362.

Nimonkar AV, Ozsoy AZ, Genschel J, Modrich P, Kowalczykowski SC et al (2008) Human exonuclease 1 and BLM helicase interact to resect DNA and initiate DNA repair. *Proceedings of the National Academy of Sciences* 105:16906-16911.

Orans J, McSweeney EA, Iyer RR, Hast MA, Hellinga HW, Modrich P *et al* Structures of human Exonuclease 1 DNA complexes suggest a unified mechanism for nuclease family. *Cell* 145:212-223.

Paull TT (2015) Mechanisms of ATM Activation. *Annual Review of Biochemistry* 84:711-738.

Petrini, I (2015) Biology of MET: a double life between normal tissue repair and tumor progression. *Annals of Translational Medicine* 3:82.

Petermann E, Woodcock M, Helleday T (2010) Chk1 promotes replication fork progression by controlling replication initiation. *Proceedings of the National Academy of Sciences* 107:16090-16095.

Pillay V, Allaf L, Wilding AL, Donoghue JF, Court NW, Greenall SA *et al* (2009) The plasticity of oncogene addiction: implications for targeted therapies directed to receptor tyrosine kinases. *Neoplasia* 11:448-458.

Ponzetto C, Bardelli A, Zhen Z, Maina F, Zonca P, Giordano S, *et al* (1994) A multifunctional docking site mediates signaling and transformation by the hepatocyte growth factor/scatter factor receptor family. *Cell* 7:261-271.

Ponzetto C, Bardelli A, Maina F, Longati P, Panayotou G, Dhand R, *et al* (1993) A novel recognition motif for phosphatidylinositol 3-kinase binding mediates its association with the hepatocyte growth factor/scatter factor receptor. *Molecular and Cellular Biology* 13:4600-4608.

Puliyappadamba VT, Chakraborty S, Chauncey SS, Li L, Hatanpaa KJ, Mickey B *et al* (2013) Opposing effect of EGFRWT on EGFRvIII-mediated NF-κB activation with RIP1 as a cell death switch. *Cell Reports* 4:764-775.

Rappold I, Iwabuchi K, Date T, Chen J (2001) Tumor suppressor p53 binding protein 1 (53BP1) is involved in DNA damage-signaling pathways. *The Journal of Cell Biology* 153:613-620.

Ropolo M, Daga A, Griffero F, Foresta M,Casartelli G, Zunino A *et al* (2009) Comparative analysis of DNA repair in stem and nonstem glioma cell cultures. *Molecular Cancer Research* 7:383-392.

Salvati M, Frati A, Russo N, Caroli E, Polli FM, Minniti, *et al* (2003) Radiation-induced gliomas: report of 10 cases and review of the literature. *Neoplasm* 60:60-67.

Sancar A, Lindsey-Boltz LA, Ünsal-Kaçmaz K, Linn S (2004) Molecular mechanisms of mammalian DNA repair and the DNA damage checkpoints. *Annual Review of Biochemistry* 73:39-85.

Sarbajna S, Davies D, West SC (2014) Roles of SLX1-SLX4, MUS81-EME1, and GEN1 in avoiding genome instability and mitotic catastrophe. *Genes & Development* 28:1124-1136.

Schaetzlein S, Kodandaramireddy NR, Ju Z, Lechel A, Stepczynska A, Lili DR *et al* (2007) Exonuclease-1 deletion impairs DNA damage signaling and prolongs lifespan of telomere-dysfunctional mice. *Cell* 130:863-877.

Schmutte C, Sadoff, Shim K, Acharya S, Fishel R (2001) The interaction of DNA mismatch repair proteins with human Exonuclease I. *The Journal of Biological Chemistry* 276:33011-33018.

Schultz LB, Chehab NH, Malikzay A, Halazonetis TD (2000) p53 binding protein 1 (53BP1) is an early participant in the cellular response to DNA double-strand breaks. *The Journal of Cell Biology* 151:1381-1390.

Skead G, Govender D (2015) Gene of the month: MET. *Journal of Clinical Pathology* 68:405-409.

Shibata A, Barton O, Noon AT, Dahm K, Deckbar D, Goodarzi AA *et al* (2010) Role of ATM and the damage response mediator proteins 53BP1 and MDC1 in the maintenance of G2/M checkpoint arrest. *Molecular and Cellular Biology* 30:3371-3383.

Shibata A, Moiani D, Arvai AS, Perry J, Harding SM, Genois M *et al* (2014) DNA double-strand break repair pathway choice is directed by distinct MRE11 nuclease activities. *Molecular Cell* 1:7-18.

Shiotani B, Zou L (2009) Single-strand DNA orchestrates an ATM-to-ATR switch at DNA breaks. *Molecular Cell* 33:547-558.

Siegel R, Miller KD, Jemal A (2016) Cancer Statistics, 2016. *CA: A Cancer Journal for Clinicians* 66:7-30.

Stupp R, Mason WP, Bent MJ, Weller M, Fisher B, Taphoorn MJ *et al* (2005) Radiotherapy plus Concomitant and Adjuvant Temozolomide for Glioblastoma. *The New England Journal of Medicine* 352:987-996.

Sun X, Zheng L, Shen B (2002) Functional alterations of human exonuclease 1 mutants identified in atypical hereditary nonpolyposis colorectal cancer syndrome. *Cancer Research* 62:6026-6030.

The Cancer Genome Atlas Research Network (2008) Comprehensive genomic characterization defines human glioblastoma genes and core pathways. *Nature* 455:1061-1068.

Tibbetts RS, Cortez D, Brumbaugh KM, Scully R, Livingston D, Elledge SJ *et al* (2000) Functional interactions between BRCA1 and the checkpoint kinase ATR during genotoxic stress. *Genes & Development* 14:2989-3002.

Tishkoff DX, Armin NS, Viars CS, Arden KC, Kolodner RD (1998) Identification of a human gene encoding a homologue of Saccharomyces cerevisiae EXO1, an exonuclease implicated in mismatch repair and recombination. *Cancer Research* 58:5027-5031.

Tkáč J, Guotai X, Adhikary H, Young JT, Gallo D, Escribano-Díaz C *et al* (2016) HELB is a feedback inhibitor of DNA end resection. *Molecular Cell* 61:405-418.

Tomimatsu N, Mukherjee B, Deland K, Kurimasa A, Bolderson E, Khanna KK *et al* (2012) Exo1 plays a major role in DNA end resection in humans and influences double-strand break repair and damaging signaling decisions. *DNA Repair (Amst)* 11:441-448.

Tomimatsu N, Mukherjee B, Hardebeck MC, Ilcheva M, Camacho CV, Harris JL *et al* (2014) Phosphorylation of EXO1 by CDKs 1 and 2 regulates DNA end resection and repair pathway choice. *Nature Communications* 5:3561.

Tsai M, Tseng H, Liu C, Chang C, Tsai C, Tsou Y *et al* (2009) Interaction of Exo1 genotypes and smoking habit in oral cancer in Taiwan. *Oral Oncology* 45:e90-e94.

Venere M, Hamerlik P, Wu Q, Rasmussen RD, Song LA, Vasanji A *et al* (2014) Therapeutic targeting of constitutive PARP activation compromises stem cell phenotype and survival of glioblastoma-initiating cells. *Cell Death and Differentiation* 21:258-269.

Verhaak RG, Hoadley KA, Purdom E, Wang V, Qi Y, Wilkerson MD *et al* (2010) An integrated genomic analysis identifies clinically relevant subtypes of glioblastoma characterized by abnormalities in PDGFRA, IDH1, EGFR and NF1. *Cancer Cell* 17:98-110.

Wang H, Chiu C, Tsai R, Kuo Y, Chen H, Wang R *et al* (2009) Association of genetic polymorphisms of EXO1 gene with risk of breast cancer in Taiwan. *Anticancer Research* 29:3897-3902.

Wang H, Shi LZ, Wong CC, Han X, Hwang PY, Truong LN *et al* (2013) The interaction of CtIP and Nbs1 connects CDK and ATM to regulate HR-mediated double-strand break repair. *PLOS Genetics* 9:e1003277.

Wang J, Wakeman TP, Lathia JD, Hjelmeland AB, Wang XF, White RR *et al* (2010) Notch promotes radioresistance of glioma stem cells. *Stem Cells* 28:17-28.

Wei K, Clark AB, Wong E, Kane MF, Mazur DJ, Parris T *et al* (2003) Inactivation of exonuclease 1 in mice results in DNA mismatch repair defects, increased cancer susceptibility, and male and female sterility. *Genes & Development* 17:603-614.

Wu Y, Berends MJ, Post JG, Mensink RG, Verlind E, Van Der Sluis T *et al* (2001) Germline mutations of EXO1 gene in patients with hereditary nonpolyposis colorectal cancer (HNPCC) and atypical HNPCC forms. *Gastroenterology* 120:1580-1597.

Wyatt HD, Sarbajna S, Matos J, West SC (2013) Coordinated actions of SLX1-SXL4 and MUS81-EME1 for Holliday junction resolution in human cells. *Molecular Cell* 52:234-247.

Xie Q, Bradley R, Kang L, Koeman J, Ascierto ML, Worschech A *et al* (2011) Hepatocyte growth factor (HGF) autocrine activation predicts sensitivity to MET inhibition in glioblastoma. *Proceedings of the National Academy of Sciences* 109:570-575.

Xu B, Kim S, Lim D, Kastan MB (2002) Two molecularly distinct G2/M checkpoints are induced by ionizing radiation. *Molecular and Cellular Biology* 22:1049-1059.

Xu N, Libertini S, Black EJ, Lao Y, Hegarat N, Walker M *et al* (2012) Cdk-mediated phosphorylation of Chk1 is required for efficient activation and full checkpoint proficiency in response to DNA damage. *Oncogene* 31:1086-1094.

Yazdi PT, Wang Y, Zhao S, Patel N, Lee EY, Qin J (2002) SMC1 is a downstream effector in the ATM/NBS1 branch of the human S-phase checkpoint. *Genes & Development* 16:571-582.

Yarden RI Pardo-Reoyo S, Sgagias M, Cown KH, Brody LC (2002) BRCA1 regulates the G2/M checkpoint by activating Chk1 kinase upon DNA damage. *Nature Genetics* 30:285-289.

Yu X, Fu S, Lai M, Baer R, Chen J (2006) BRCA1 ubiquitinates its phosphorylation-dependent binding partner CtIP. *Genes & Development* 20:1721-1726.

Yun MH, Hiom K (2009) CtiP-BRCA1 modulates the choice of DNA double-strand-break repair pathway throughout the cell cycle. *Nature* 459:460-463.

Zhou Y, Caron P, Legube G, Paull TT (2014) Quantitation of DNA double-strand break resection intermediates in human cells. *Nucleic Acids Research* 42:e19.